

Technical Report

Foryd Harbour Lifting Bridge

Deck Structural Design Report

Report No: 3073-8001

Issue B

Gurit Project No: GU3073

Author: Stefano Casini

Business Unit:	Technology	Department:	Engineering
Classification:	Commercial in Confidence	Approved by:	M Hobbs

Issue and Amendments

ISSUE	AMENDMENTS	DATE	CHECKED	APPROVED
P1	Preliminary Design	19 May 2011	Mark Hobbs	Mark Hobbs
A	Detailed Design	16 July 2012	Mark Hobbs	Mark Hobbs
B	Open bridge results added. Local calculations added	30 November 2012	Mark Hobbs	Mark Hobbs

AM Structures

Ramboll

File

This document is confidential and is the property of Gurit (UK) Ltd ("the company"). It is for the sole use of the person to whom it is addressed and may not be copied or otherwise reproduced or stored in any retrievable system or divulged to any third party or used for manufacture or any other purpose without, in each case, the prior written consent of the company.

All advice, instruction or recommendation is given in good faith but the Company only warrants that advice in writing is given with reasonable skill and care. No further duty or responsibility is accepted by the Company. All advice is given subject to the terms and conditions of sale (the Conditions) which are available on request from the Company or may be viewed at the Company's website: <http://www.gurit.com/>

The Company strongly recommends that Customers make test panels and conduct appropriate testing of any goods or materials supplied by the Company to ensure that they are suitable for the Customer's planned application. Such testing should include testing under conditions as close as possible to those to which the final component may be subjected. The Company specifically excludes any warranty of fitness for purpose of the goods other than as set out in writing by the Company. The Company reserves the right to change specifications without notice and Customers should satisfy themselves that information relied on by the Customer is that which is currently published by the Company on its website. Any queries may be addressed to the Technical Department.

Content

1.	Introduction	4
2.	Structural Arrangement	6
3.	Material Properties	7
4.	Design Specifications	8
4.1	Load Combinations	8
5.	Finite Element Analysis	10
5.1	Views of FE Model.....	10
5.2	Modelling for Static Analysis.....	12
5.2.1	<i>Restraints.....</i>	12
5.2.2	<i>Suspension System and Hydraulic Ram</i>	13
5.2.3	<i>Cable Pretension</i>	13
5.2.4	<i>Mass</i>	13
5.2.5	<i>Wind Load.....</i>	14
5.3	Modelling for Dynamic Analysis.....	16
6.	Results and Verifications	18
6.1	Global Response	18
6.1.1	<i>Bridge in Closed Position.....</i>	18
6.1.2	<i>Bridge in Partially Open Position</i>	33
6.1.3	<i>Bridge in Fully Open Position</i>	38
6.2	Local Analysis of the Deck.....	41
6.3	Design of Bridge Details	45
6.3.1	<i>Interface at the hinge end</i>	45
6.3.2	<i>Lifting pin support structure</i>	49
	References	51
	Bibliography	51

1. Introduction

This report summarises the structural analysis carried out for the detailed design of the bridge deck of the Foryd Harbour Lifting Bridge, a footbridge due to be built across the Clwyd River, at its estuary, in the County Denbighshire, Wales. This report should be read in conjunction with the Deck Structural Design Specifications [1].

The general layout of the bridge is shown in Figure 1.

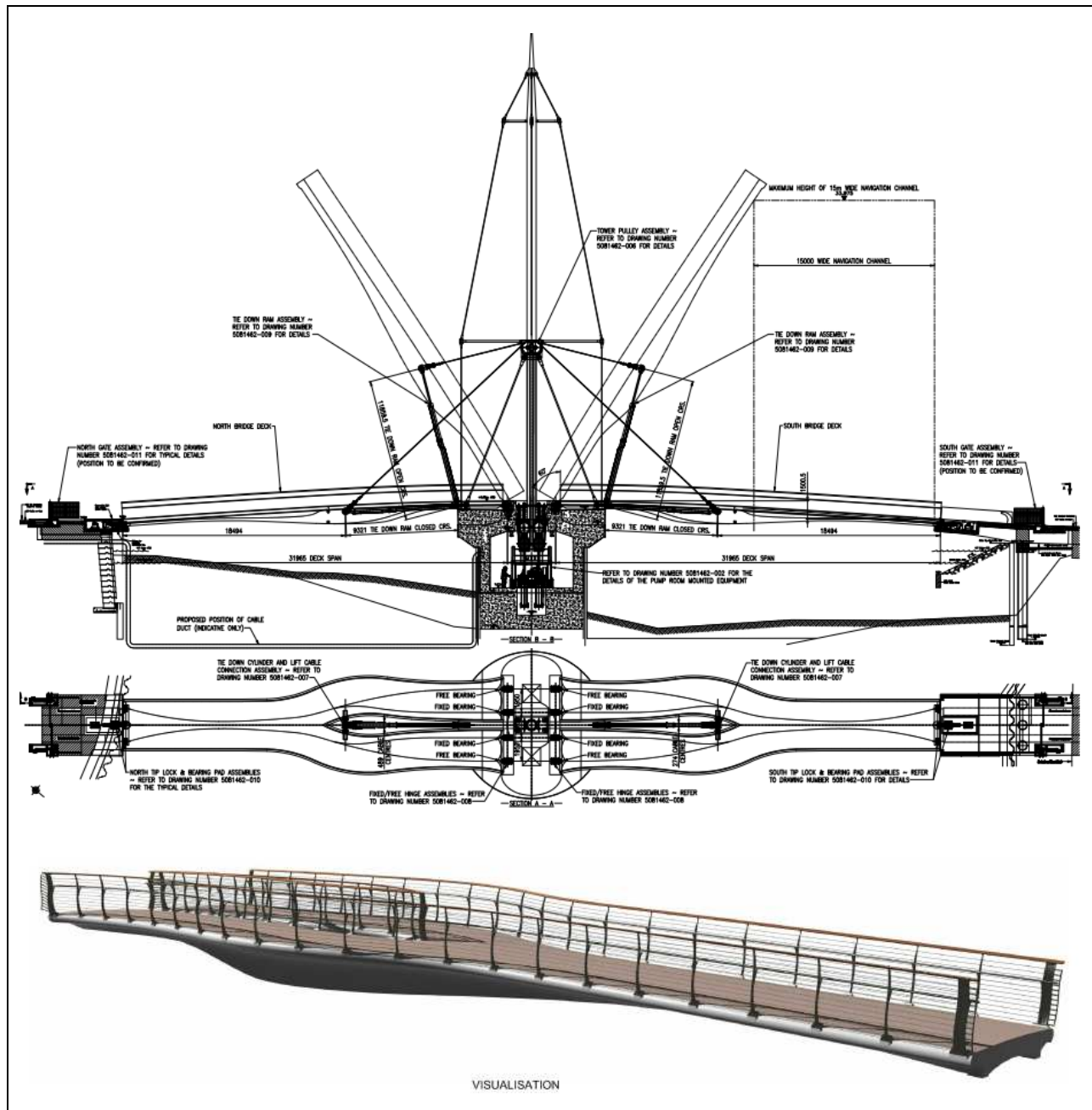


Figure 1: Bridge layout (by Ramboll)

The bridge is a two-span moveable bridge, with the two 32 metres spans rotating about the central support by means of a hinge and a lifting cables and winches system.

There is a couple of lifting cables per each span, which have also the function of support for bridge in closed position, contributing to the stiffness of the bridge deck. The support offered by the cable is provided through a steel tube which transfers the load from the cables to the bridge deck.

The cross-section of the bridge deck varies along the span. Typical sections are reported in Figure 2.

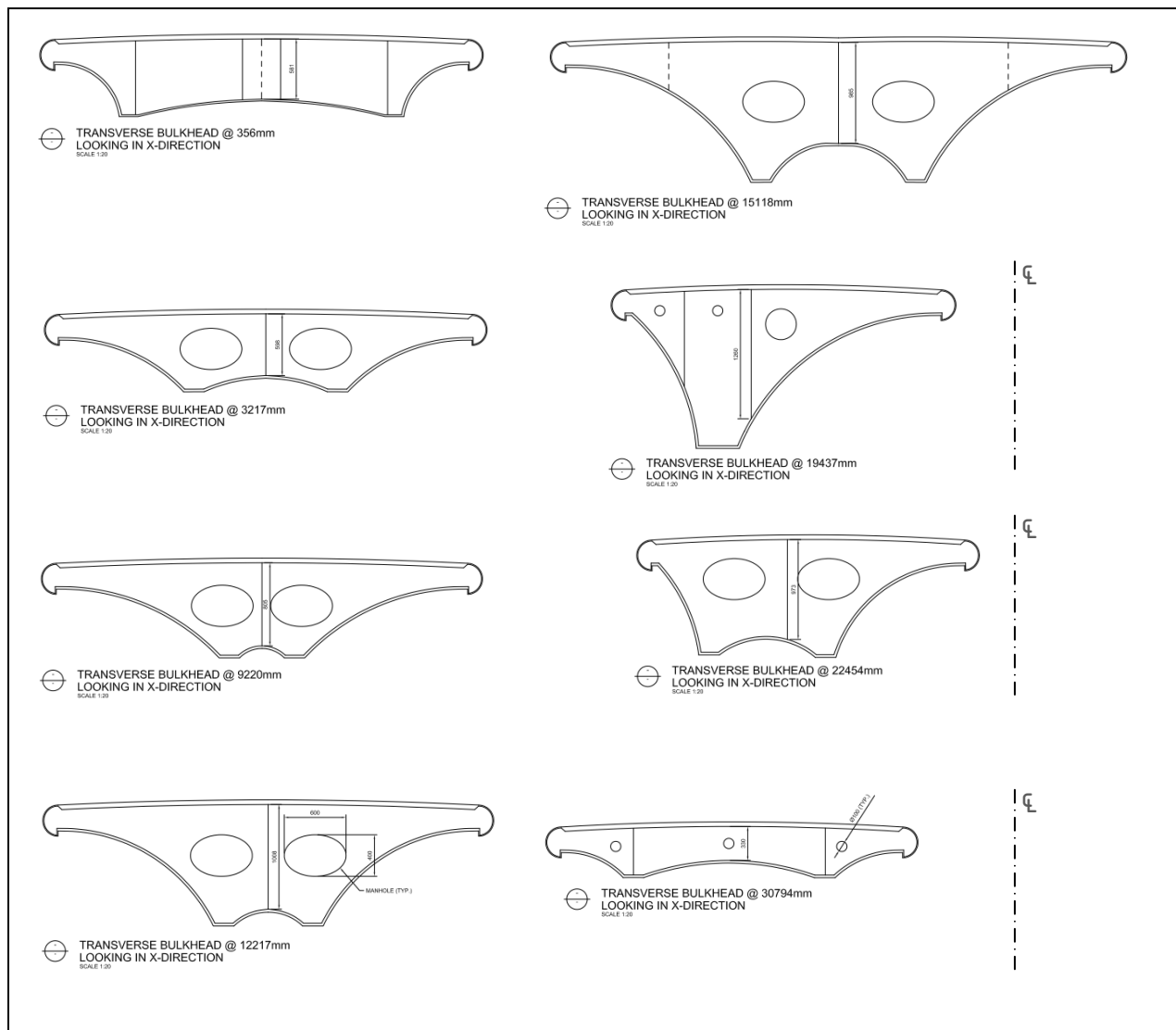


Figure 2: Typical cross-sections

The bridge deck will be realized with moulded FRP components, mainly in the form of sandwich panels, consisting in two wet laminated / vacuum consolidated epoxy glass laminates separated by and bonded to a foam core panel.

Each of the two spans of the bridge will be manufactured in two parts to be transported and bolted together along the centre line on site.

The bridge is supposed to be partially or fully open (respectively at 30° and 60°) only with Wind Force up to 7. For stronger wind the bridge will remain closed. In the open positions, the bridge deck is anchored to the concrete plinth of central pylon by means of a hydraulic ram, connected to the steel tube and hinged at the two ends. In closed position, the bridge is locked down by means of a horizontal piston and wheel system at the landwards end.

This report details the design work carried out on the moulded FRP bridge deck. The design of the mast, lifting system and substructures is carried out by others.

2. Structural Arrangement

The arrangement of the main structural components (such as top deck, deck soffit, longitudinal diaphragms and bulkheads) is shown in Figure 3. Where possible, access to the inside of the bridge deck shell has been provided by manholes on the top deck and in the internal structure. Where the depth of the bridge deck does not allow physical access, holes for visual inspection have been provided instead.

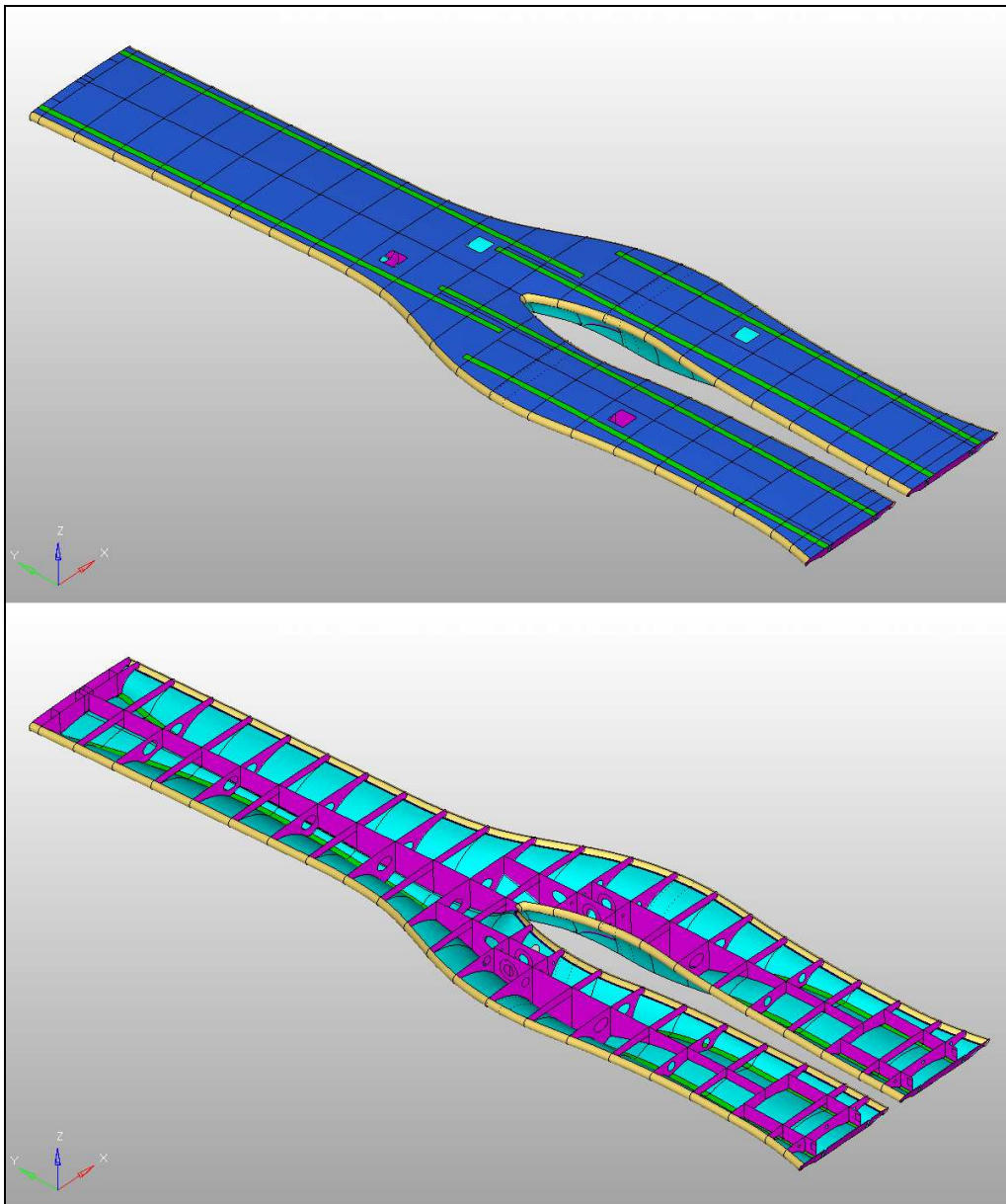


Figure 3: Structural arrangement

The structure is to be manufactured from wet laminated / vacuum consolidated epoxy glass laminates. For the laminates reference should be made to the construction. Unidirectional carbon fibres in the form of 200/250 mm strips will also be introduced as additional longitudinal reinforcement on the top deck and along the deepest points of the deck soffit.

3. Material Properties

The following material properties have been assumed in this analysis:

		QE990 Emfv QUADAXIAL GLASS	XE905 Emfv BIXIAL GLASS (*)	UE800 Emfv UNIDIR. GLASS	UCHSC400 Emfv UNIDIR. CARBON	M80 Corecell
Fibre Volume Fraction Vf		44%	42%	44%	44%	-
Longitudinal Modulus Ex	N/mm ²	17.210	8.922	33.180	101.445	37
Transverse Modulus Ey	N/mm ²	17.210	8.922	7.740	5.990	37
Shear Modulus Gxy	N/mm ²	6.490	8.702	2.910	3.070	25
Poisson's Ratio vxy	-	0.355	0.599	0.267	0.333	0.4
Shear Modulus Gxz/Gyz	N/mm ²	2.910	2.790	2.910	3.070	25
Bolt Bearing Strength	N/mm ²	200	-	-	-	-
Ultimate Longitudinal Tensile Strength	N/mm ²	258	-	597	1030	8
Ultimate Longitudinal Compressive Strength	N/mm ²	198	-	398	629	20
Ultimate Transverse Tensile Strength	N/mm ²	258	-	35	27	8
Ultimate Transverse Compressive Strength	N/mm ²	198	-	116	90	20
Ultimate In-plane Shear Strength	N/mm ²	156	130.5	34.9	36.8	-
Ultimate Interlamina Shear Strength	N/mm ²	35	33.5	34.9	36.8	-
Density	kg/m ³	1.752	1.729	1.764	1.412	85
Layer Thickness	mm	0.86	0.83	0.70	0.51	var.
Core Shear Strength	N/mm ²	-	-	-	-	0.96

(*) The values reported refer to fibres at +/- 45°

Table 1: Material properties

4. Design Specifications

For a complete description of the design specifications, including characteristic loads, load partial factors, load combination factors and design requirements, reference should be made to the Deck Structural Design Specifications [1].

Currently there are no specific design standards in force in the UK for the design of FRP structures. However, the design of the bridge deck was carried out in accordance with the Limit State methodology as employed in the Eurocodes [2][3][4][5].

Material partial factors were taken from "EuroComp Design Code and Handbook for Structural Design of Polymer Composites" [6] which is based on the Limit State design methodology.

4.1 Load Combinations

The load combinations investigated are reported below together with the related partial load factors and combination factors according to the Eurocode and as reported in the Deck Structural Design Specifications.

SLS 1 (permanent before locking):	self-weight + surfacing + parapets (only hinged end restraints and cable)
SLS 2 (permanent after locking):	self-weight + surfacing + parapets (only end restraints)
SLS 3 (permanent in service):	self-weight + surfacing + parapets + prestress (cable + end restraints and horizontal bridge)
SLS 4 (irreversible):	permanent in serv + traffic 1 ^(*)
SLS 5 (irrev.):	permanent in serv + traffic 2 ^(**)
SLS 6 (irrev.):	permanent in serv + traffic 3 ^(***)
SLS 7 (irrev.):	permanent in serv + traffic 4 ^(****)
SLS 8 (reversible):	permanent in serv + 0.40 traffic 1
SLS 9 (rev.):	permanent in serv + 0.40 traffic 2
SLS 10 (rev.):	permanent in serv + 0.40 traffic 3
SLS 11 (rev.):	permanent in serv + 0.40 traffic 4
SLS 12 (irrev.):	permanent in serv + (transverse + downward wind)
SLS 13 (irrev.):	permanent in serv + (transverse + uplift wind)

(*) Traffic 1 = pedestrian load over entire deck

(**) Traffic 2 = pedestrian load over landwards side span

(***) Traffic 3 = pedestrian load over pylon side span

(****) Traffic 4 = pedestrian load over half deck along the entire span

SLS 14 (permanent during lifting):	self-weight + surfacing + parapets (restraints at the lifting points)
SLS 15 (permanent with partially open bridge):	self-weight + surfacing + parapets (cable and hydraulic ram + hinged end restraints and bridge open at 30°)
SLS 16 (partially open bridge – irrev.):	perm partially open + (transverse + downward wind)
SLS 17 (partially open bridge – irrev.):	perm partially open + (transverse + uplift wind)
SLS 18 (partially open bridge – irrev.):	perm partially open + longitudinal wind
SLS 19 (partially open bridge – irrev.):	perm partially open – longitudinal wind
SLS 20 (permanent with fully open bridge):	self-weight + surfacing + parapets (cable and hydraulic ram + hinged end restraints and bridge open at 60°)
SLS 21 (fully open bridge – irrev.):	perm fully open + longitudinal wind
SLS 22 (fully open bridge – irrev.):	perm fully open – longitudinal wind
ULS 1:	1.35 perm in serv + 1.35 traffic 1 + 1.55 x 0.30 (transv wind + downward wind)
ULS 2:	1.35 perm in serv + 1.35 traffic 2 + 1.55 x 0.30 (transv wind + downward wind)
ULS 3:	1.35 perm in serv + 1.35 traffic 3 + 1.55 x 0.30 (transv wind + downward wind)
ULS 4:	1.35 perm in serv + 1.35 traffic 4 + 1.55 x 0.30 (transv wind + downward wind)
ULS 5:	1.35 parapet loads
ULS 6:	1.35 perm + 1.50 service vehicle
ULS 7 (partially open bridge):	1.35 perm partially open + 1.55 transv wind + 1.55 downward wind
ULS 8 (partially open bridge):	0.95 perm partially open + 1.55 transv wind + 1.55 uplift wind
ULS 9 (partially open bridge):	1.35 perm partially open + 1.55 longitudinal wind
ULS 10 (partially open bridge):	0.95 perm partially open - 1.55 longitudinal wind
ULS 11 (fully open bridge):	1.35 perm fully open + 1.55 longitudinal wind
ULS 12 (fully open bridge):	0.95 perm fully open - 1.55 longitudinal wind

5. Finite Element Analysis

Due to the complexity and challenging shape of the bridge, an FE model was built, based on a 3D geometric model provided by AM Structures and using shell elements with composite material constitutive laws. Given the symmetry, only one main span was modelled.

The model, counting about 84150 shell elements (see Figure 5), was built and analysed by the FEA package HyperWorks. A less refined mesh (46600 elements) was used for the dynamic analysis.

5.1 Views of FE Model

The main views of the FE model are shown below.

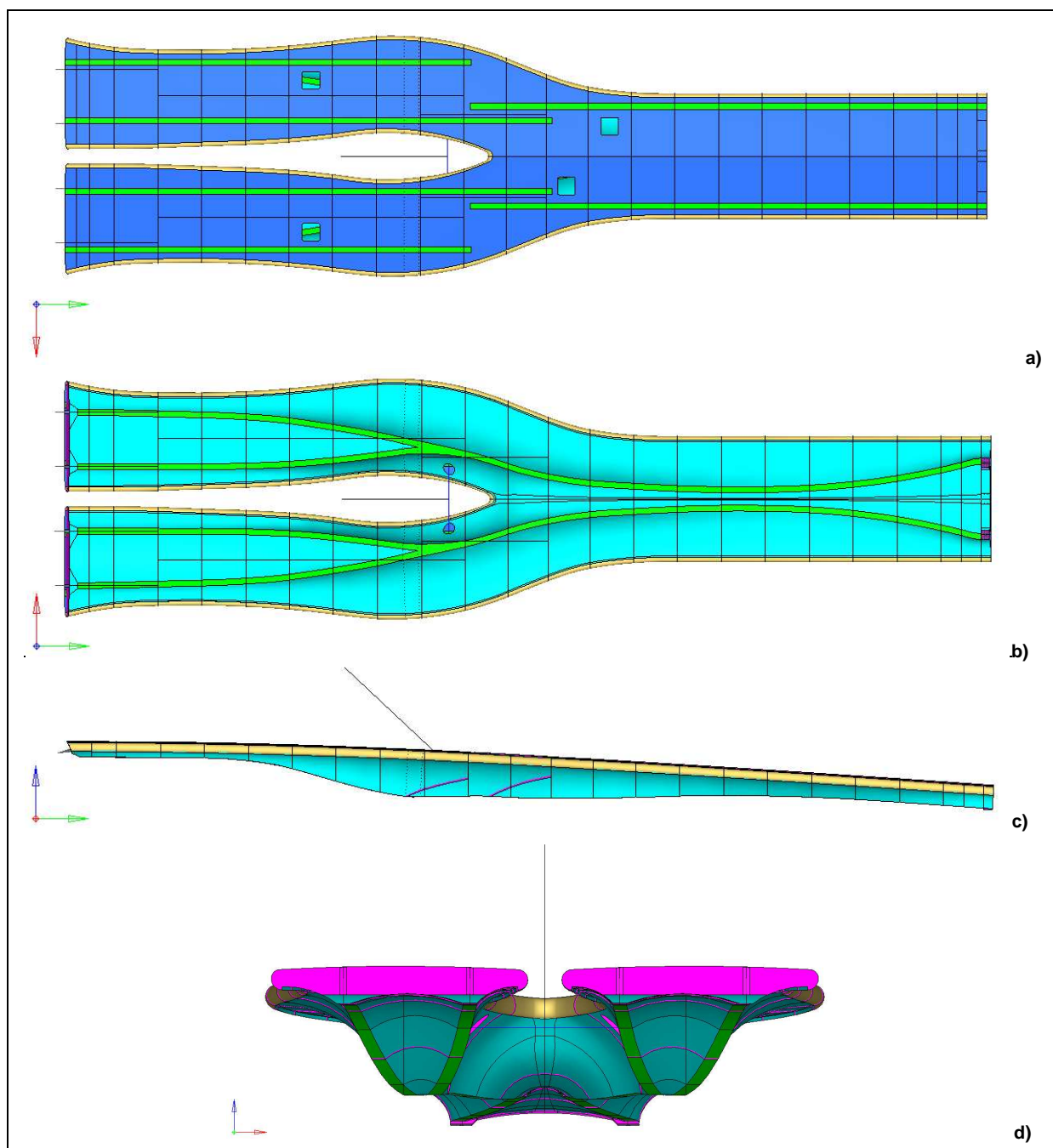


Figure 4: FE model – Geometry: a) top view; b) bottom view; c) profile; d) front view from the pylon

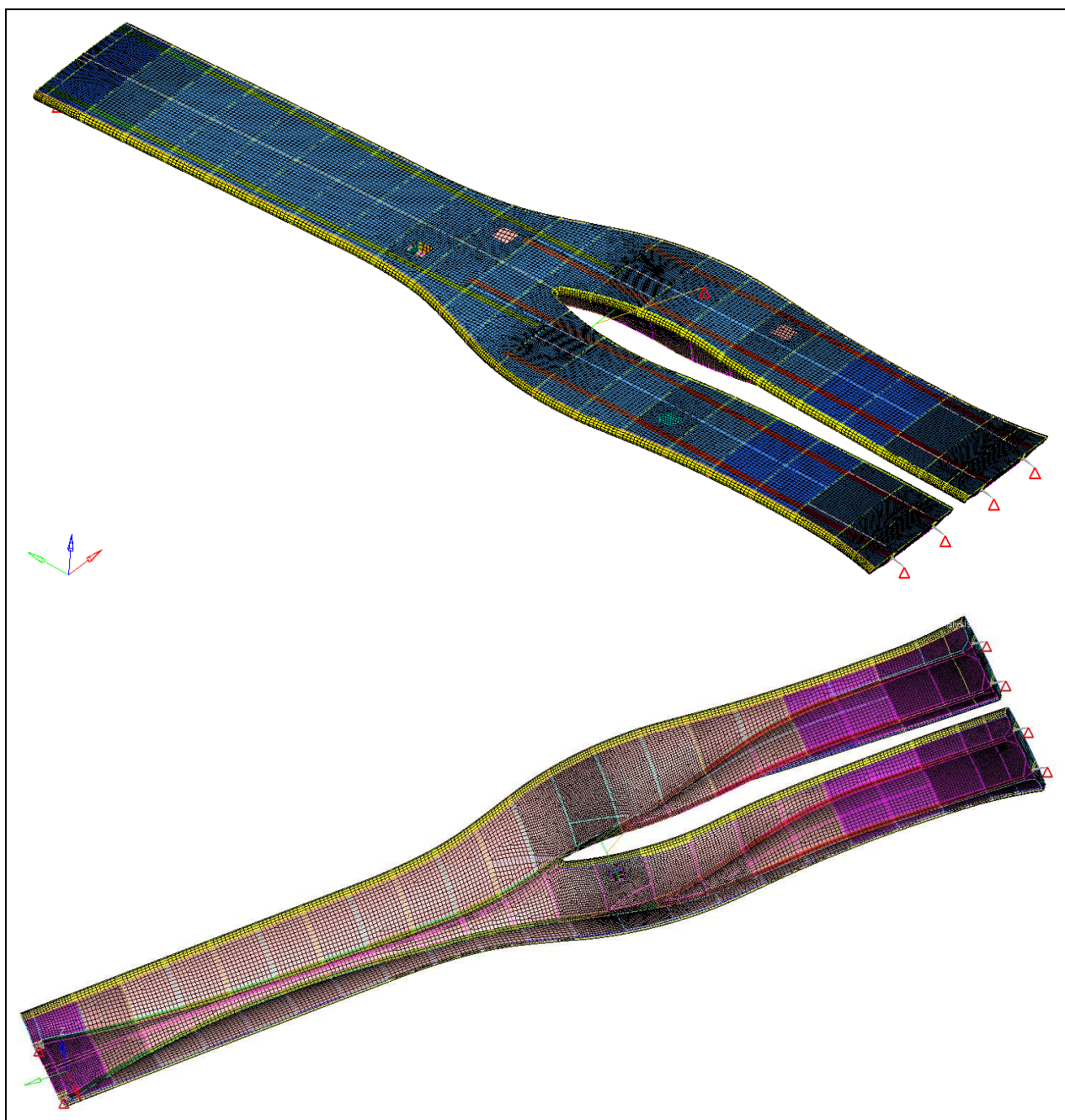


Figure 5: FE Model for Static Analysis – Mesh

5.2 Modelling for Static Analysis

As mentioned, the bridge deck was modelled by means of shell elements (i.e. 2D finite elements), which were given the properties of the related composite panels.

The bridge was modelled in the following three positions (see Figure 6):

- closed bridge (for crossing of pedestrians)
- partially open at 30° (for navigation of boats)
- fully open at 60° (for navigation of boats)

with the open position depending on wind speed.

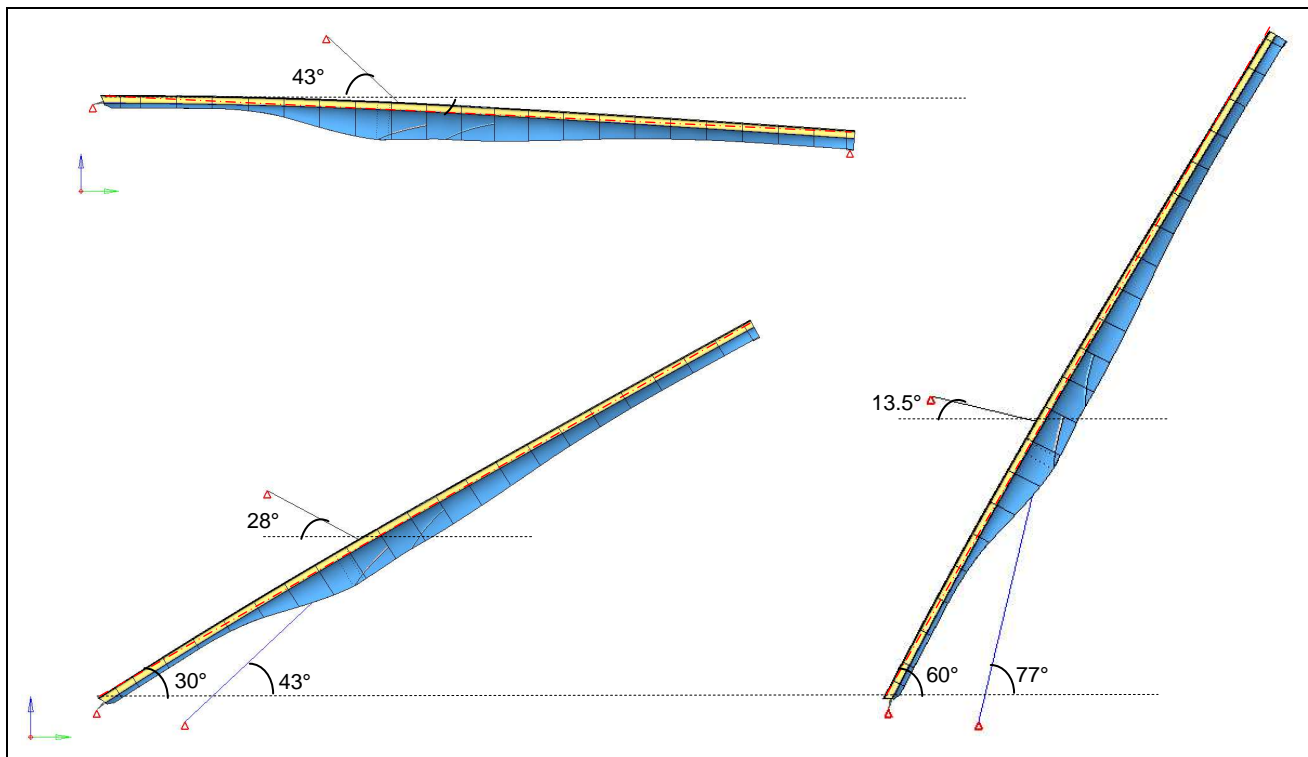


Figure 6: Bridge positions

5.2.1 Restraints

In the closed position, the following three restraint conditions were considered:

- before locking: bridge supported at the hinge and by the cable and subjected only to permanent loads
- during locking: bridge supported at the two ends (i.e. loose cable) and subjected only to permanent loads
- in service: bridge supported at the two ends and by the cable under all load combinations with pretensioned cable

In the open position the bridge was considered supported at the hinged end and by the cable and also tied down by the hydraulic ram.

At the hinged end the bridge was assumed to have all the degrees of freedom restrained except for the rotation about the pin axle (i.e. the x-axis in the global coordinate system). At the opposite end, in addition to the rotation about the x-axis, the longitudinal translation was also released.

5.2.2 Suspension System and Hydraulic Ram

The modelling of the interaction of the bridge deck with the suspension system and the hydraulic ram tie down system was simplified by the introduction of springs of equivalent stiffness. The values of the stiffness were provided by Ramboll [7] and included in the Deck Structural Design Specifications [1].

The equivalent stiffness of the cable used in the analysis is:

- closed bridge position (hydraulic valves open): $2 \times 2641 \text{ kN/m}$
- partially open (30° - hydraulic valves closed and ram stroke 1 m): $2 \times 3010 \text{ kN/m}$
- fully open (60° - hydraulic valves closed and ram stroke 2.8 m): $2 \times 3350 \text{ kN/m}$

The equivalent stiffness of the hydraulic ram was obtained from a graph provided by Ramboll, reporting the ram stroke vs. stiffness. The values for the different positions of the bridge deck are as follows:

- closed bridge position (hydraulic valves open): $\sim 0 \text{ kN/m}$
- partially open (30° - hydraulic valves closed and ram stroke 1 m): $13\,000 \text{ kN/m}$
- fully open (60° - hydraulic valves closed and ram stroke 2.8 m): $110\,000 \text{ kN/m}$

5.2.3 Cable Pretension

With the closed bridge in service (i.e. after locking) a pretension of the cable was introduced in order to reduce the net deflections and avoid the cable from becoming loose under uplift wind. In particular, a pretension of 195.5 kN was considered, being this the pretension that leads to zero reactions at the tip (i.e. all permanent loads being supported by the cable and hinge) and agreed as the maximum pretension allowed.

5.2.4 Mass

In addition to the structural mass automatically accounted for by the software, an additional non-structural mass (about 28.5%) was distributed in the model to take into account extra material used in joints, overlaps etc. The total mass of the bridge was *8.89 tonnes*.

Note that, in carrying out the dynamic analysis (see Par. 5.3), in addition to the above mass of the composite materials, superimposed dead loads such as surfacing and parapets have been taken into account by means of additional non-structural mass distributed respectively over the top deck and along the deck edge. This led the total mass in the FE model used in the dynamic analysis to be *12.48 tonnes*.

5.2.5 Wind Load

Coherently with the Eurocode and Ramboll's directions, the characteristic values of the wind pressures reported in the Deck Structural Design Specifications [1] were considered as the values of uniform pressure distribution over the projected area of the bridge deck orthogonally to the wind direction, both for transverse and longitudinal wind (see Figure 7).

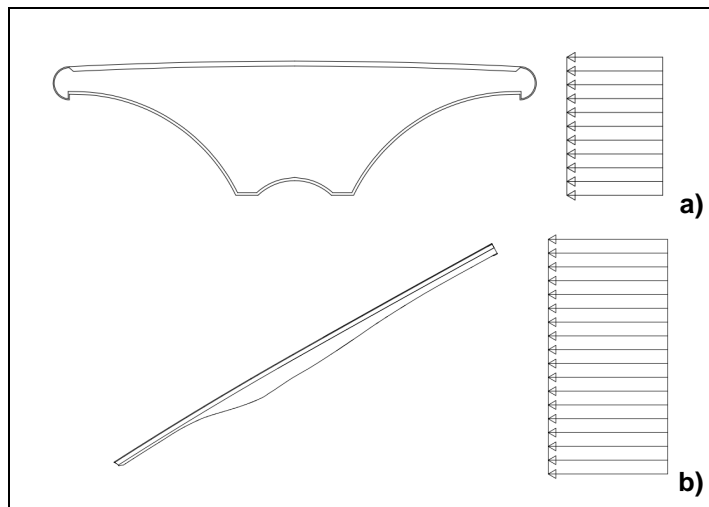


Figure 7: Wind pressure distribution: a) transverse wind; b) longitudinal wind

The lateral projected area of the bridge deck is:

$$A_{p,transv} = 29.8 \text{ m}^2$$

and therefore the total transverse wind load is:

- closed bridge: $F_{w,transv} = p_{w,transv} A_{p,transv} = 1.43 \text{ kN/m}^2 29.8 \text{ m}^2 = 42.61 \text{ kN}$
- open bridge 30°: $F_{w,transv} = p_{w,transv} A_{p,transv} = 1.43 \text{ kN/m}^2 29.8 \text{ m}^2 = 42.61 \text{ kN}$
- open bridge 60°: $F_{w,transv} = p_{w,transv} A_{p,transv} = 0.75 \text{ kN/m}^2 29.8 \text{ m}^2 = 22.35 \text{ kN}$

The transverse wind load was applied by an approximate quadratic pressure distribution over the windward and leeward lateral panels, having the resultant equal to the above total loads and centroid coincident with the centroid of the projected area (see Figure 8).

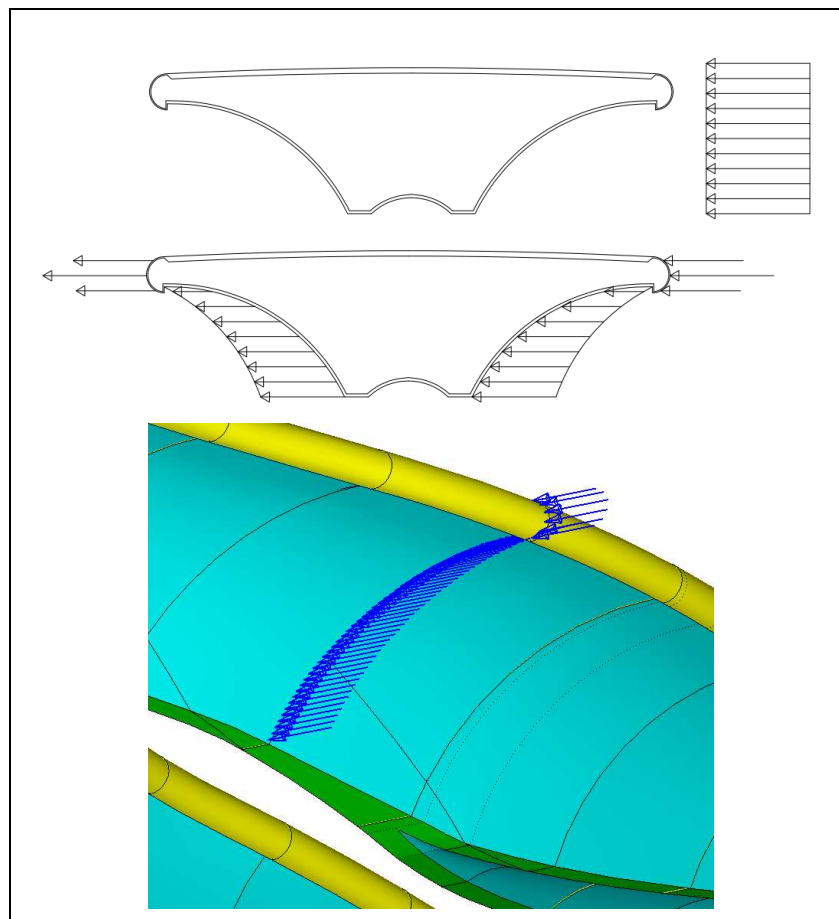


Figure 8: Equivalent transverse wind pressure distribution

The downwards and uplift wind load, associated with the transverse wind load, were simply applied as a uniform pressure over the top deck.

Similarly, the longitudinal wind load was applied in both the directions simply as a force uniformly distributed over the top deck but in the horizontal direction. The projected area of the top deck is:

- open bridge 30°: $A_{p, \text{long}} = 82.3 \text{ m}^2$
- open bridge 60°: $A_{p, \text{long}} = 142 \text{ m}^2$

and therefore the total longitudinal wind load is:

- open bridge 30°: $F_{w, \text{long}} = p_{w, \text{long}} A_{p, \text{long}} = 0.84 \text{ kN/m}^2 82.3 \text{ m}^2 = 69.2 \text{ kN}$
- open bridge 60°: $F_{w, \text{long}} = p_{w, \text{long}} A_{p, \text{long}} = 0.84 \text{ kN/m}^2 142 \text{ m}^2 = 119 \text{ kN}$

5.3 Modelling for Dynamic Analysis

As shown in Par. 6.1.1.6, the vertical vibration frequency is less than the limit set by the Eurocode and therefore a fully dynamic analysis (i.e. time-dependent analysis) was required in order to assess the maximum vertical acceleration and compare it with the maximum acceptable value (see BS EN 1990: 2002+A1: 2005, A2.4.3.2). As the lateral natural frequency was above the limit set by Eurocode there was no need to verify the lateral stability of the bridge.

Although the verification of comfort criteria was required only with reference to the vertical vibrations, given the importance of this limit state and the complexity of the topic, the dynamic response of the bridge has been also analysed with reference to the first torsional mode as the frequency of this mode was close to the first vertical mode and this mode has the potential to be excited by vertical actions of pedestrians.

The dynamic analysis was carried out using the dynamic models of pedestrian loads and associated comfort criteria defined in NA to BS EN 1991-2: 2003, NA.2.44. For each of the two natural frequencies:

- vertical vibrations: $f = 3.29 \text{ Hz}$
- torsional vibrations: $f = 3.73 \text{ Hz}$

the dynamic response of the bridge was assessed under the passage of groups of pedestrians walking and running and also under crowded conditions.

As per the Deck Structural Design Specifications [1], the bridge was assumed to be of class B and for it the Eurocode recommends the following values for the size of groups of pedestrians and for the crowd density (see Table NA.7):

- walking group: $N = 4 \text{ persons}$
- jogging group: $N = 1 \text{ persons}$
- crowd density: $\rho = 0.4 \text{ persons/m}^2$ (walking)

The dynamic actions representing the passage of a group of pedestrians consist in a vertical pulsating force F (N), moving across the span of the bridge at a constant speed v_t , represented by the following function of time t :

$$F(t) = F_0 k(f) [1 + \gamma (N-1)]^{0.5} \sin(2 \pi f t)$$

where:

- | | |
|----------|--|
| N | is the number of persons in the group (see above) |
| F_0 | is the reference amplitude (walking: 280 N; jogging: 910 N – see Table NA.8) |
| f | is the natural frequency of the vibration mode in consideration |
| $k(f)$ | is a corrective coefficient (see below) |
| γ | is a reduction factor to allow for unsynchronized actions within groups and crowds (pedestrian groups: 0.225; crowd: 0.028 – see Figure NA.9 with effective span = 32 m) |
| v_t | is the pedestrian crossing speed (walking 1.7 m/s; jogging: 3 m/s – see Table NA.8) |

For simplicity, the above force was applied along a path running along the edge of the deck, which is a conservative assumption.

The pulsating force representing the walking group of pedestrians along the bridge was:

- vertical vibrations mode: $F(t) = 116 \sin(20.5 t) N \quad (k(3.26 \text{ Hz}) = 0.32)$
- torsional vibrations mode: $F(t) = 130 \sin(23.4 t) N \quad (k(3.73 \text{ Hz}) = 0.36)$

The pulsating force representing the jogging group of pedestrians along the bridge was:

- vertical vibrations mode: $F(t) = 273 \sin(20.5 t) N \quad (k(3.26 \text{ Hz}) = 0.30)$
- torsional vibrations mode: $F(t) = 109 \sin(23.4 t) N \quad (k(3.73 \text{ Hz}) = 0.12)$

In the following figure is reported the graph from the Eurocode [5] which provides the relationships between $k(f)$ and f .

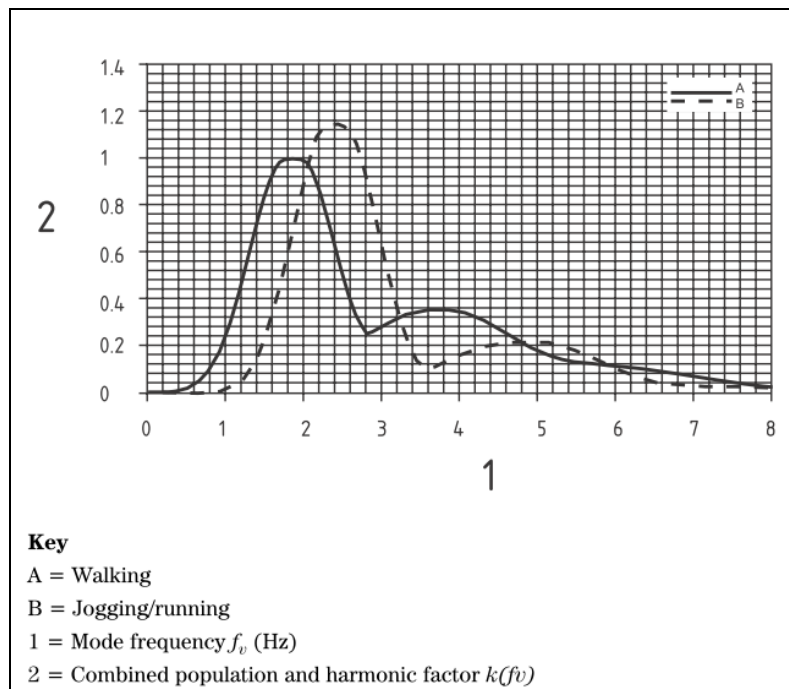


Figure 9: Relationships between $k(f)$ and f
(from NA to BS EN 1991-2: 2003, Figure NA.8)

Crowded conditions are modelled by a vertical pulsating distributed load w (N/m^2), applied to the deck for a sufficient time so that steady state conditions are achieved, as follows:

$$w(t) = 1.8 (F_0/A) k(f) (\gamma N/\lambda)^{0.5} \sin(2\pi f t)$$

where:

$A = 163 m^2$ is the deck area

$N = \rho A = 65$

$\lambda = 0.634$ is a further corrective coefficient (see NA.2.44.5 with effective span = 32 m)

The distributed load $w(t)$ was applied uniformly over the entire deck when considering the vertical mode of vibration and in opposite direction on the two halves of the deck when considering the torsional mode of vibration.

The pulsating distributed force representing the crowded condition was:

- vertical vibrations mode: $w(t) = 274 \sin(20.5 t) N/m^2$ ($k(3.26 \text{ Hz}) = 0.32$)
- torsional vibrations mode: $w(t) = 308 \sin(23.4 t) N/m^2$ ($k(3.73 \text{ Hz}) = 0.36$)

A structural damping of 2% was assumed based on previous Gurit's experiences and measurements [8].

6. Results and Verifications

A selection of the output of the analysis is reported in the following paragraphs together with the related structural checks. The verification of the global response of the bridge is first presented (Par. 6.1) followed by the design of details (Par. 6.2).

6.1 Global Response

6.1.1 Bridge in Closed Position

6.1.1.1 SLS 1 – Permanent loads before locking

The maximum deflection of the bridge deck under permanent loads with bridge in horizontal position immediately before locking the landward end (i.e. with only hinged end restraints and cable) was 244.5 **mm** (i.e. **span/130**). A contour of the vertical displacements plotted on a deformed model is reported in the following figure.

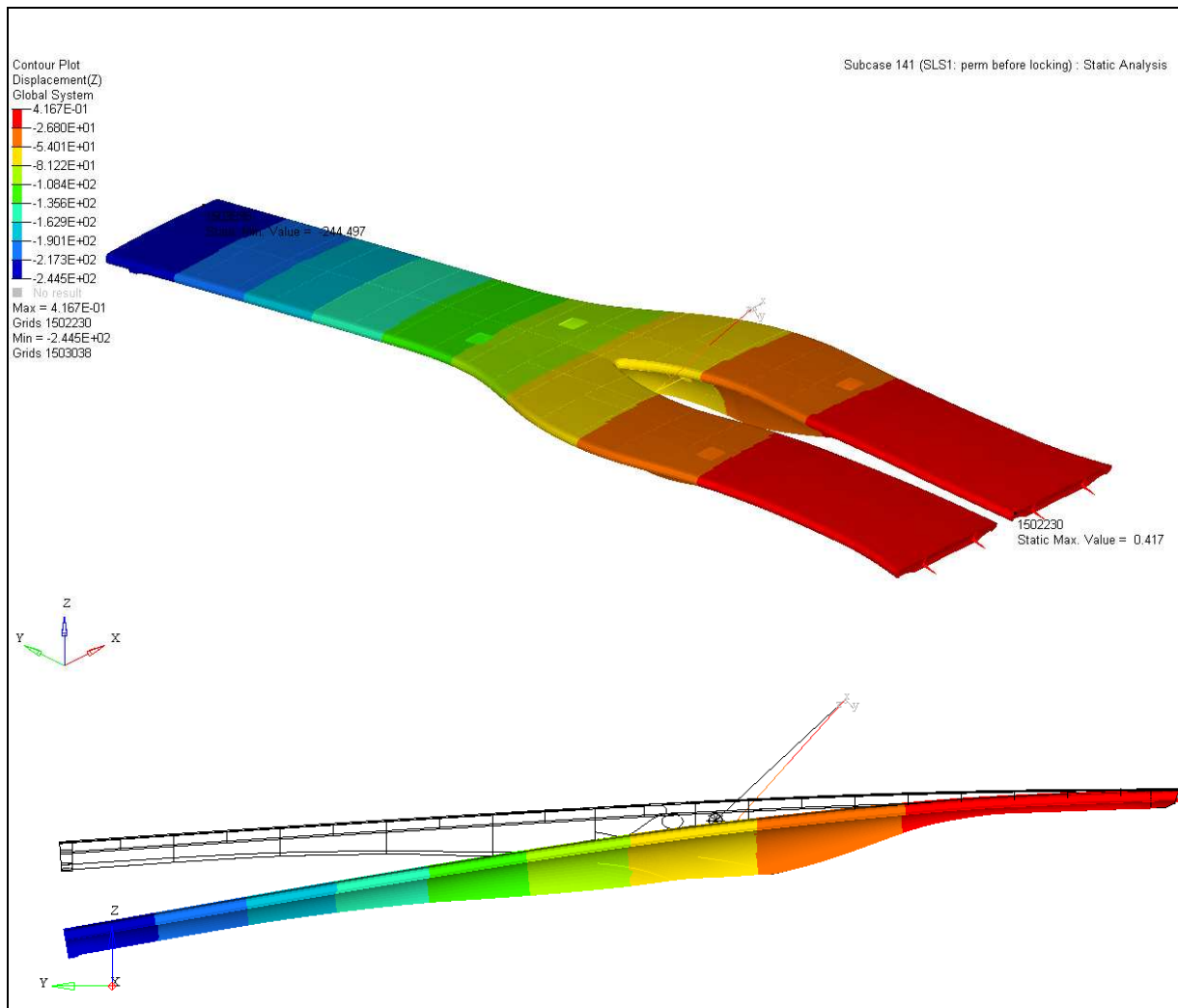
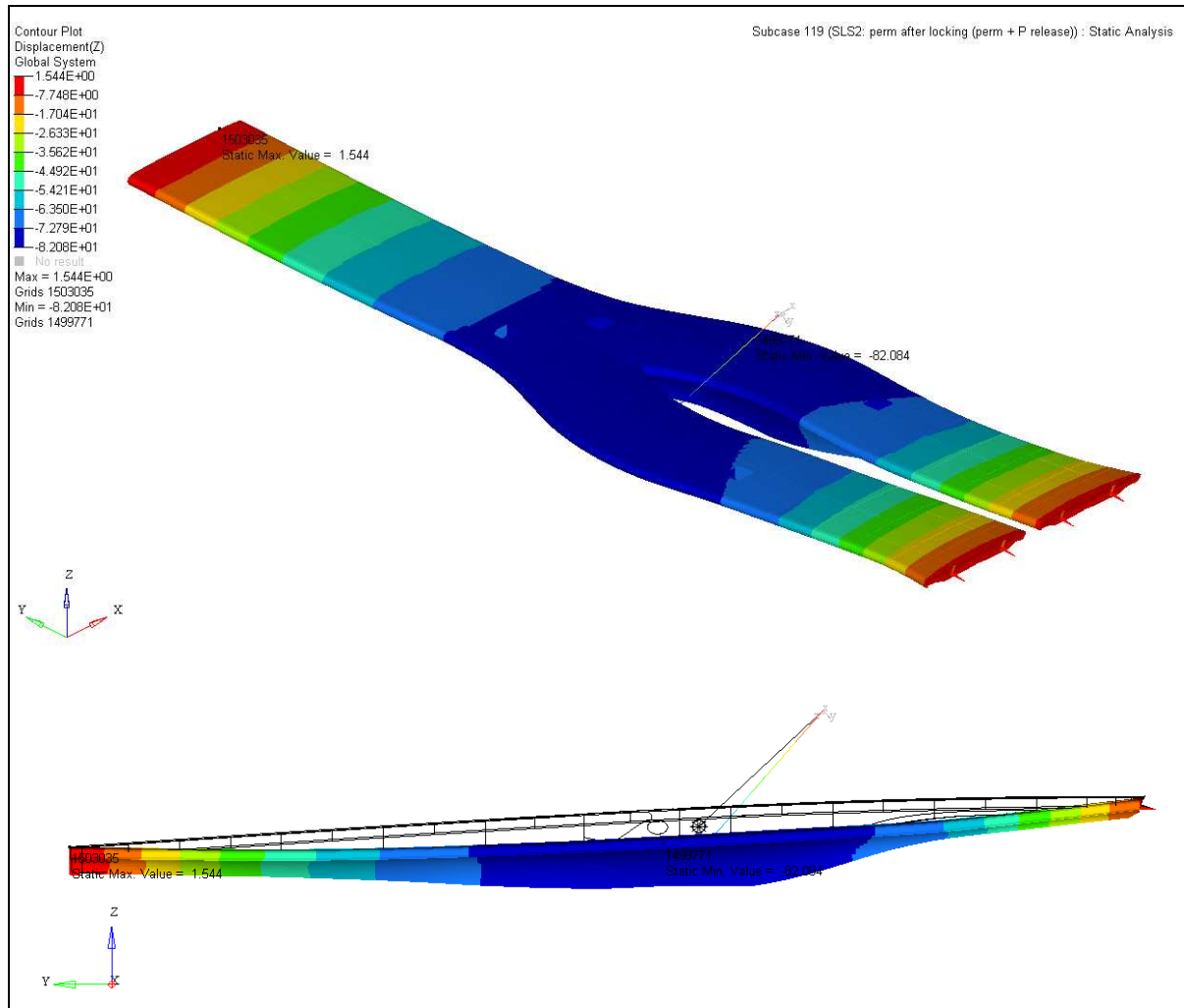


Figure 10: Vertical displacement contour at the SLS 1 (amplification coefficient 10)

The tensile strain is about 0.16%, which is less than the allowable transverse strain in uni-directional plies and therefore no further check of the strains is required.

6.1.1.2 SLS 2 – Permanent loads after locking

The maximum deflection of the bridge deck under permanent loads with bridge in horizontal position immediately after locking the landward end and before tensioning the cable resulted of **82 mm** (i.e. **span/390**). A contour of the vertical displacements plotted on a deformed model is reported in the following figure.



**Figure 11: Vertical displacement contour at the SLS 2
(amplification coefficient 10)**

The maximum tensile strain is about 0.23%, which is less than the allowable transverse strain in unidirectional plies and therefore no further check of the strains is required.

6.1.1.3 SLS 3 – Permanent loads in service

The maximum deflection of the bridge deck under permanent loads with bridge in horizontal position and after pulling the cable up to induce in it a tension force of 195.5 kN was of 43 mm. This force was assessed as that necessary to relieve the supports at the tip of the bridge from carrying any permanent load (from Figure 12 it results that the total reaction at the tip is basically zero). As it is shown in Par. 6.1.1.9, this pretension prevents the cable from becoming loose due to the uplift wind (at the ULS).

A contour of the vertical displacements plotted on a deformed model is reported in the following figure.

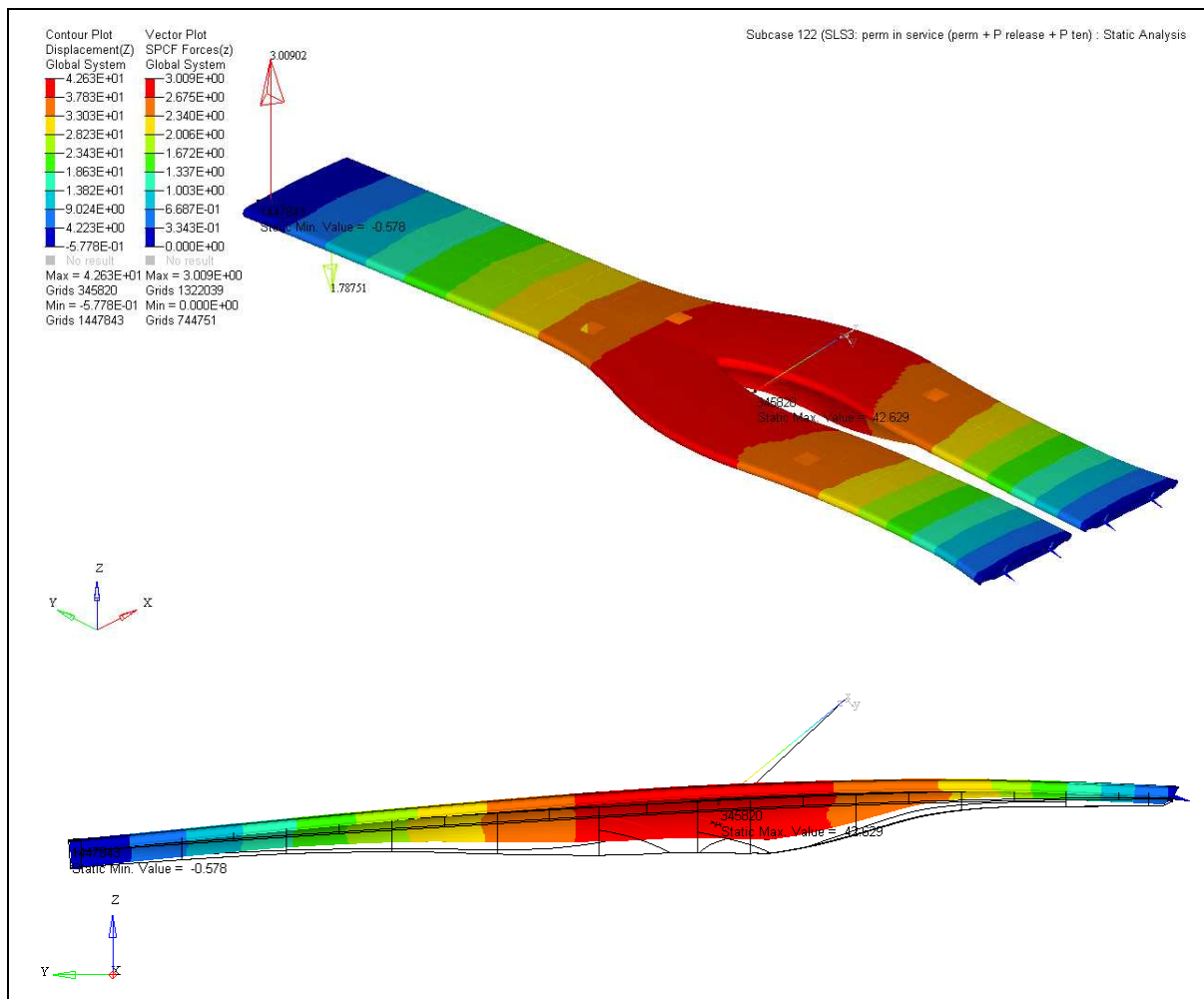


**Figure 12: Vertical displacement contour at the SLS 3
(amplification coefficient 10)**

The maximum tensile strain is about 0.16%, which is less than the allowable transverse strain in uni-directional plies and therefore no further check of the strains is required.

6.1.1.4 Deformations and Strains under traffic loads

The check of the maximum tensile strains against the allowable strains was carried out with reference to the load combinations SLS4, SLS5 and SLS6, which represent characteristic combinations to be used for irreversible limit states such as matrix cracking. With the exclusion of stress concentrations around the hinge (which will be dealt in detail in Par. 6.2), the maximum tensile strains of 0.27% are less than the allowable strain of 0.4% and therefore no further checks of the strains are required (see Figure 13).

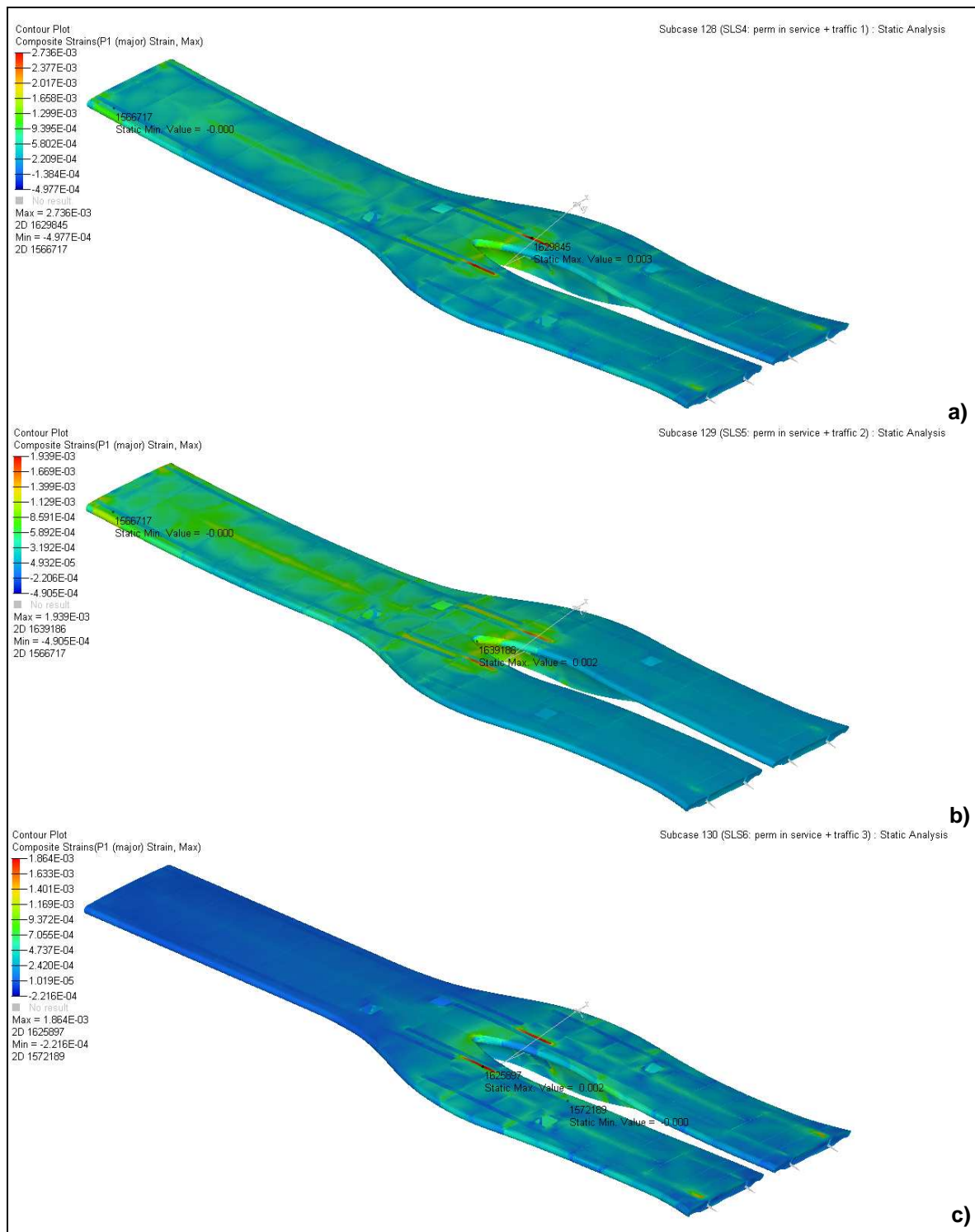


Figure 13: Maximum tensile strains under traffic load in characteristic conditions:
a) SLS4; b) SLS5; c) SLS6
(plotted on deformed shape with amplification coefficient 5)

Although the Eurocodes do not provide explicit limits in terms of deflections, these have been assessed in the SLS7, SLS8 and SLS9, which represent frequent combinations to be used for reversible limit states, such as deflections.

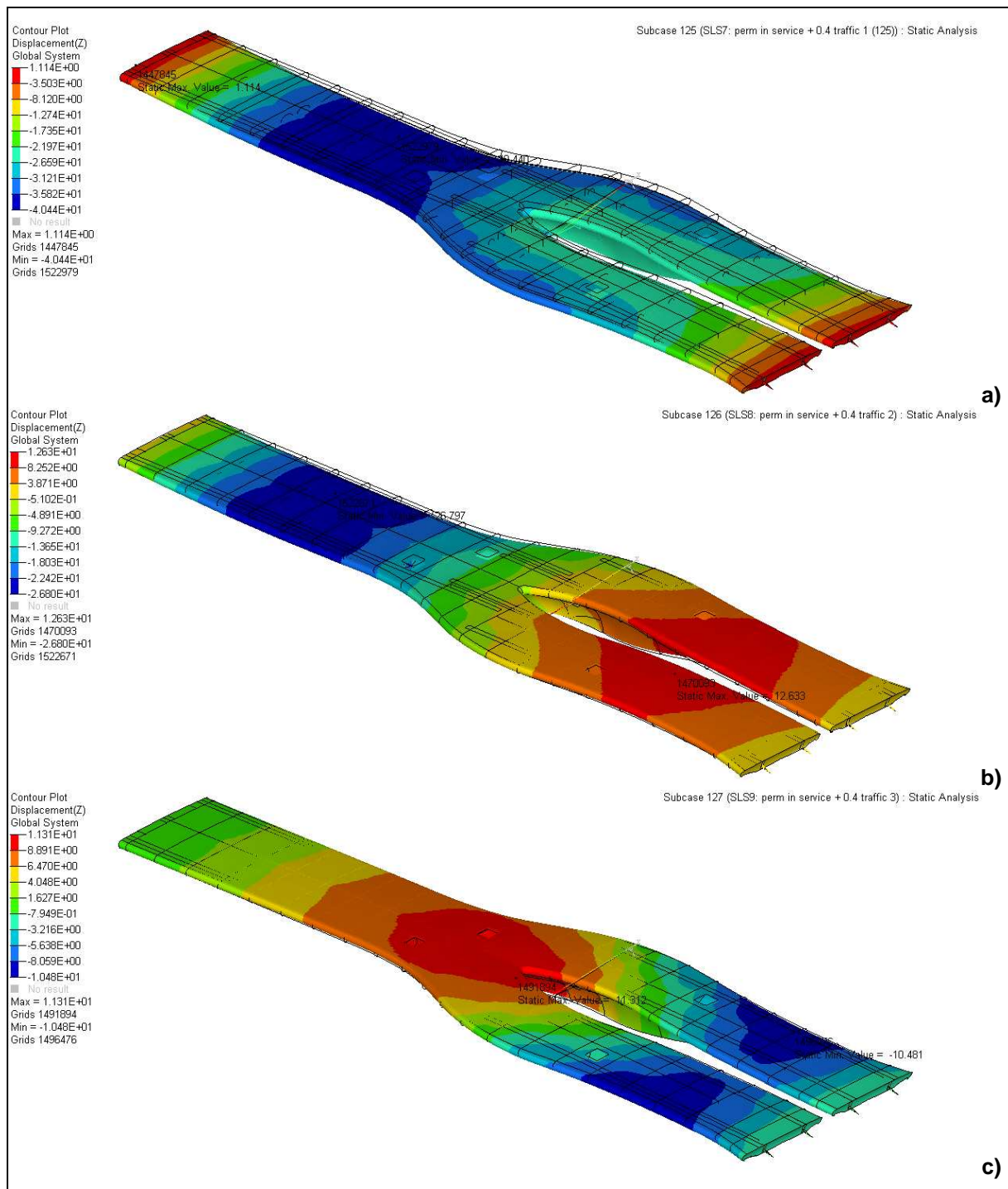


Figure 14: Vertical displacement contour under traffic loads: a) SLS 7; b) SLS 8; c) SLS 9 (amplification coefficient 10)

The maximum deflection of the bridge deck under traffic load was 40.4 mm (SLS7: traffic load over the entire deck), that is equal to span/792 (under the characteristic value for the traffic load more commonly considered by previous codes, the maximum deflection increases to 147.5 mm, i.e. span/217).

6.1.1.5 SLS10: Permanent loads + Transverse wind + downward wind

The effect of the transverse wind load and associated downward wind load in terms of deflections of the bridge deck is here reported (see Figure 15).

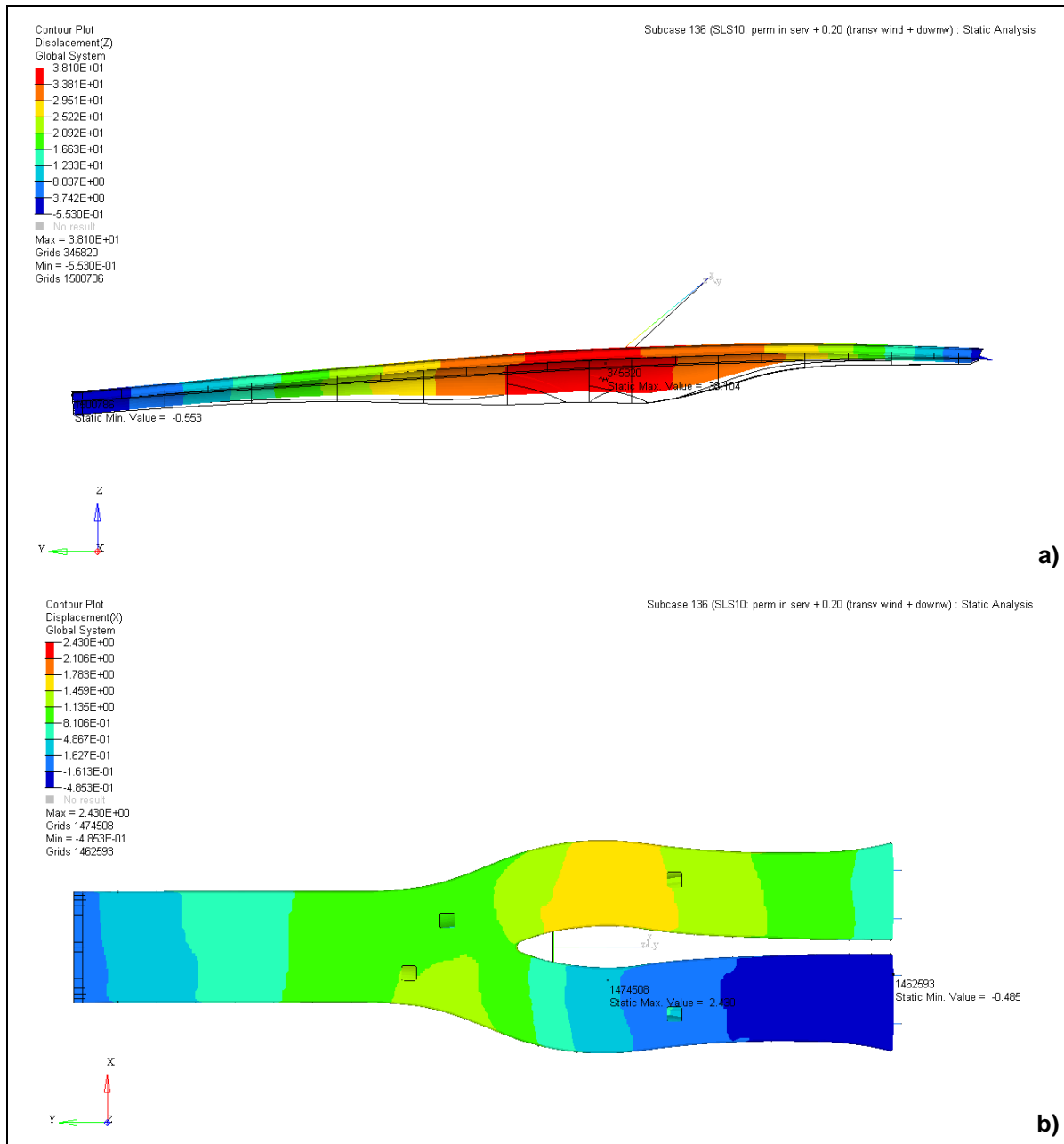


Figure 15: Displacement contour under transverse wind + downward wind:
a) vertical displacements; b) horizontal displacements
(amplification coefficient 10)

As it can be seen, the maximum horizontal displacement of the bridge deck is small, 2.4 mm. Once again, it should be noted that no explicit limits are defined by the Eurocodes in terms of maximum deflections.

6.1.1.6 Natural frequencies and dynamic analysis under pedestrian loads

The deformed shapes corresponding to the first four modes of vibration are reported in Figure 16.

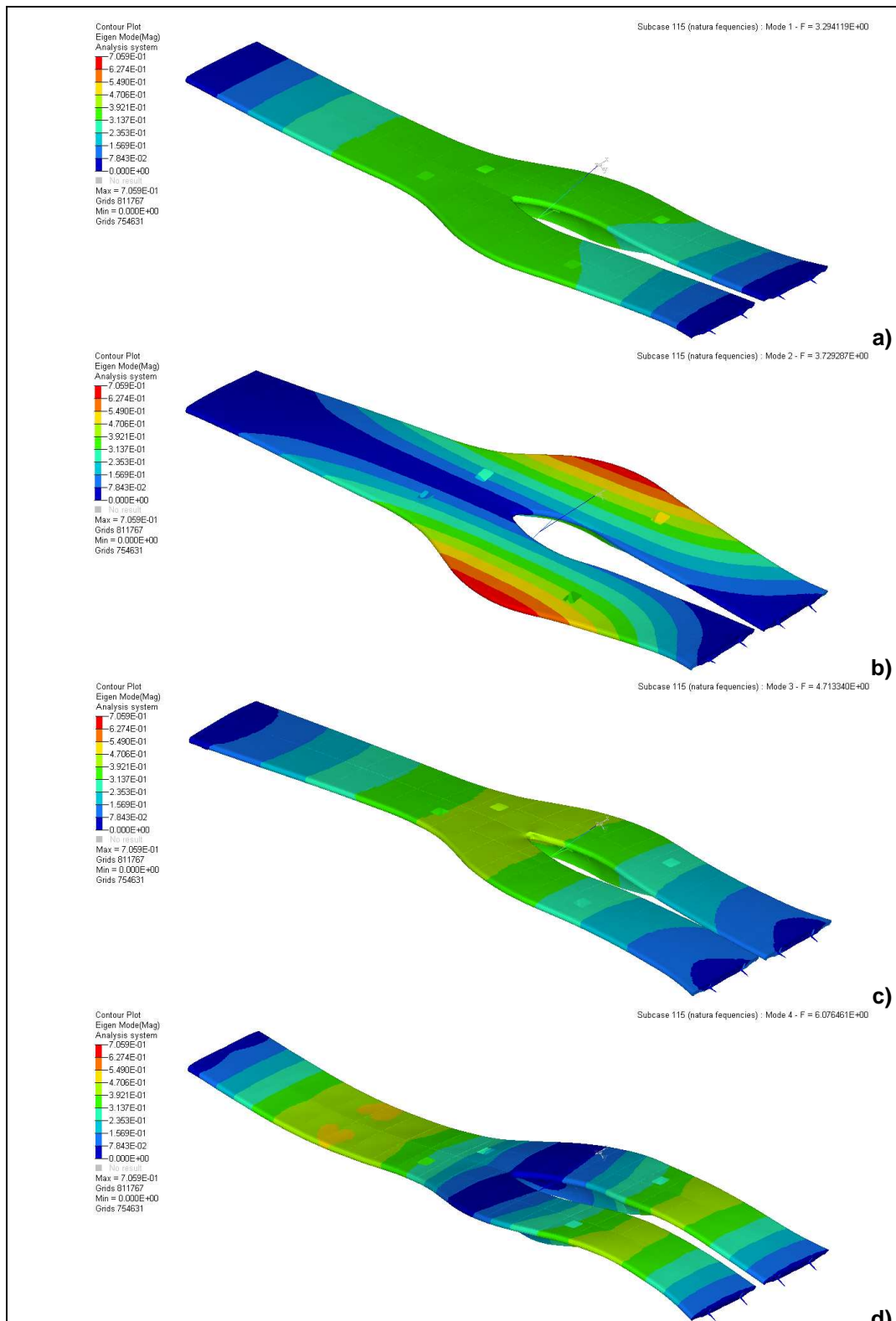


Figure 16: Modes of vibration: a) Mode 1: vertical vibrations; b) Mode 2: torsional vibrations; c) Mode 3: lateral vibrations; d) Mode 4: secondary vertical vibrations

The natural frequencies are as follows:

- vertical vibrations (first mode): $3.3 \text{ Hz} < 5 \text{ Hz}$
- torsional vibrations (second mode): $3.7 \text{ Hz} > 2.5 \text{ Hz}$
- lateral vibrations (third mode): $4.7 \text{ Hz} > 2.5 \text{ Hz}$
- vertical vibrations (second mode): $6.1 \text{ Hz} > 5 \text{ Hz}$

Therefore, according to BS EN 1990: 2002+A1: 2005, Par. A2.4.3.2, cl. 2, the verification of comfort criteria is required only with reference to the vertical vibrations. However, given the importance of this limit state and the complexity of the topic, the dynamic response of the bridge has been also analysed with reference to the torsional vibrations. See Par. 5.3 for details regarding the dynamic modelling.

The maximum acceleration due to jogging groups of pedestrians was found when considering the vertical mode of vibrations ($f = 3.3 \text{ Hz}$). Some results from this analysis are shown in Figure 17.

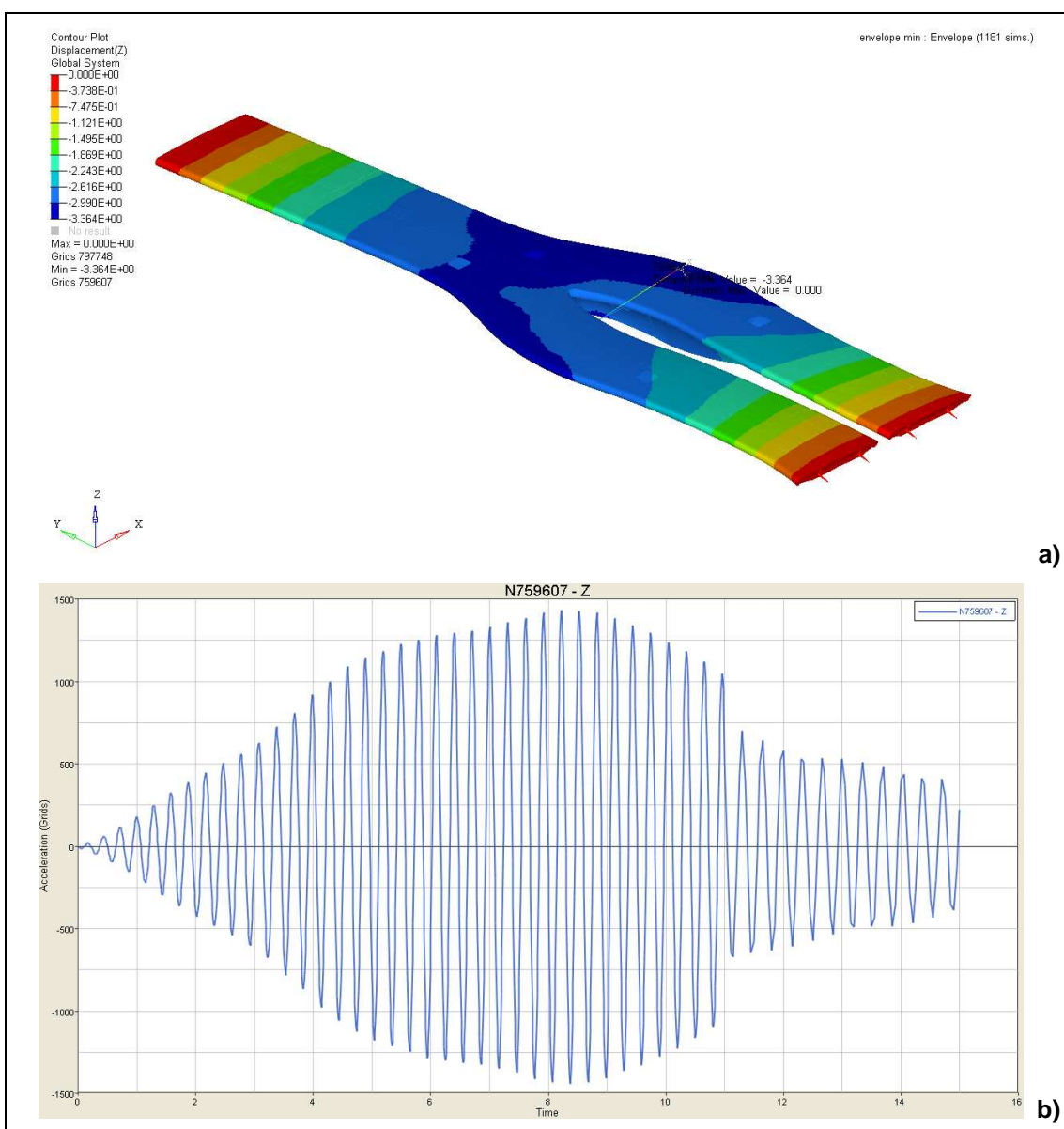


Figure 17: Running group of pedestrians: a) Envelope of minimum vertical displacements; b) Acceleration time-history at the point of minimum vertical displacement

The maximum vertical acceleration is expected at the point of minimum vertical displacement and it is equal to about 1.45 m/sec^2 which is less than the allowable acceleration of 1.89 m/sec^2 .

The maximum acceleration due to walking groups of pedestrians was actually found when considering the torsional mode of vibrations (note that the amplitude of the pulsating force corresponding to the natural frequency of torsional mode of vibration is higher than that corresponding to the vertical mode of vibration – see Par. 5.3). Some results from this analysis are shown in Figure 18.

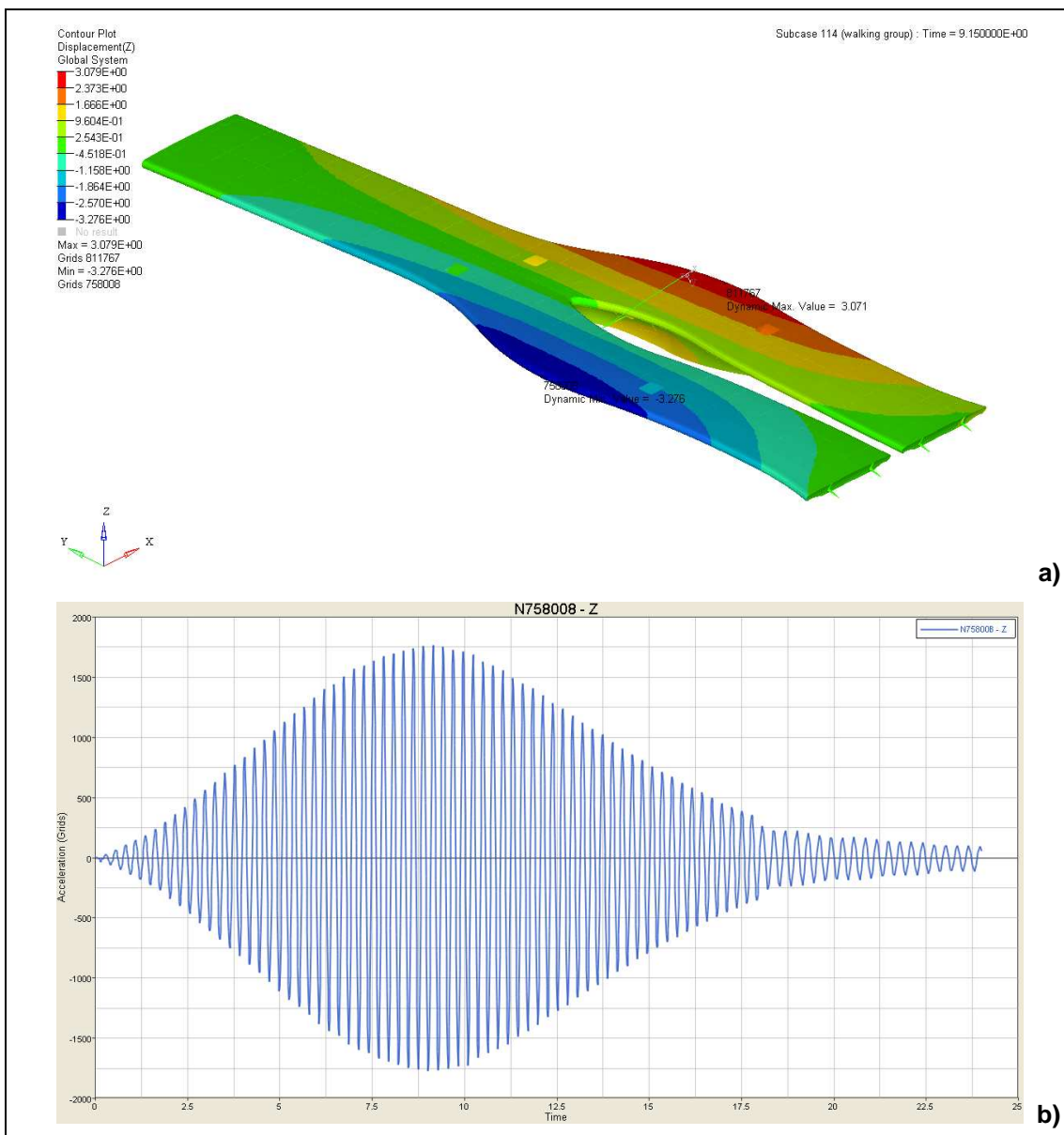


Figure 18: Walking group of pedestrians: a) Contour of vertical displacements at the time of minimum displacement; b) Acceleration time-history at the point of minimum vertical displacement

The maximum vertical acceleration is expected at the point of minimum vertical displacement and it is equal to about 1.75 m/sec^2 which is still less than the allowable acceleration of 1.89 m/sec^2 .

Note how the contour plot of the minimum vertical displacements shows how the applied pulsating load essentially induces torsional vibrations in the bridge having the same frequency as the natural frequency of the torsional mode of vibration.

Finally, the maximum acceleration due to walking crowd in steady state conditions was found when considering the vertical mode of vibrations ($f = 3.3 \text{ Hz}$). Some results from this analysis are shown in Figure 19.

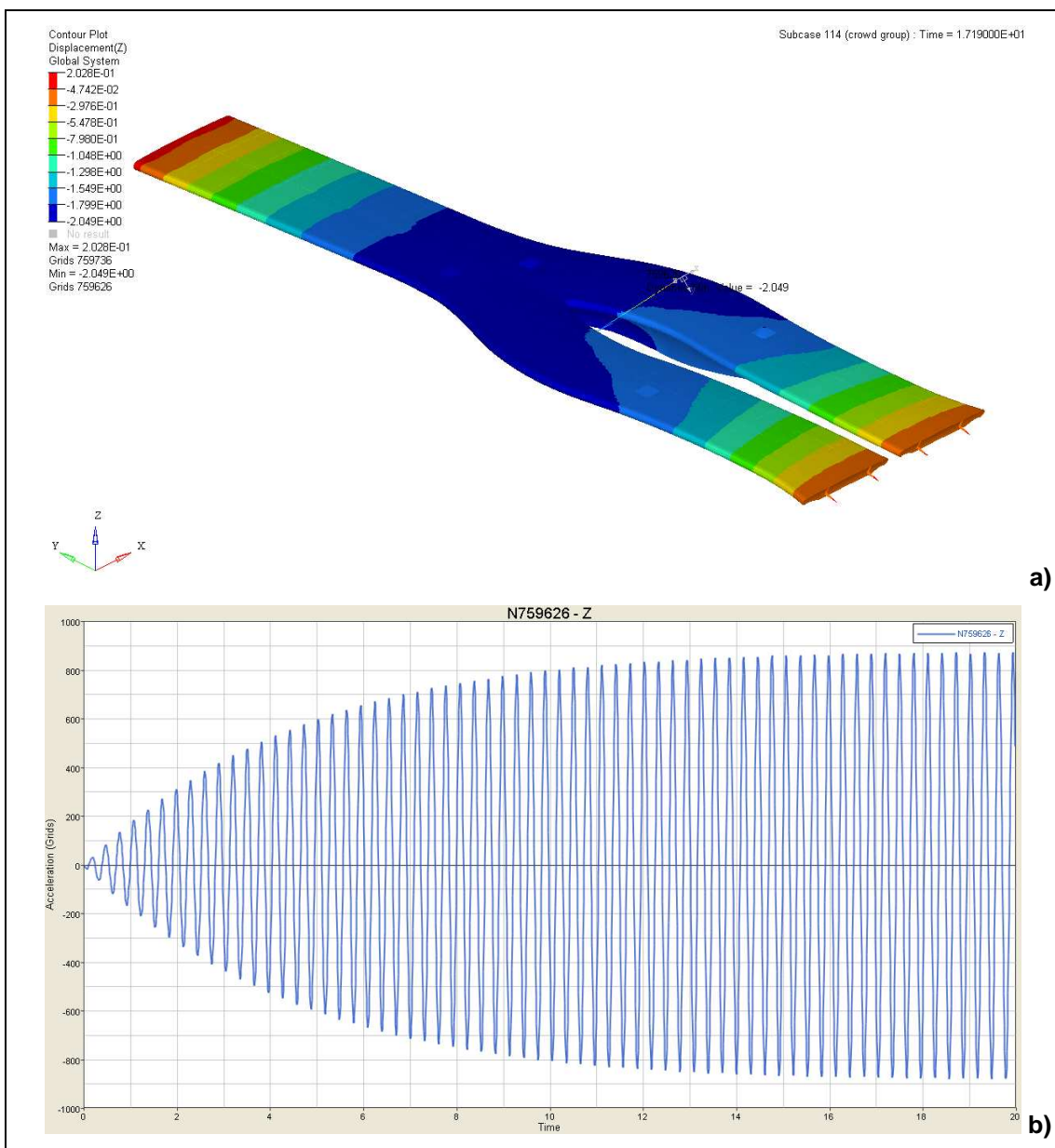


Figure 19: Crowd loading: a) Contour of vertical displacements at the time of minimum displacement in steady conditions; b) Acceleration time-history at the point of minimum vertical displacement

The maximum vertical acceleration is expected at the point of minimum vertical displacement and it is equal to about 0.9 m/sec^2 , which is less than the allowable acceleration of 1.89 m/sec^2 .

A summary of the accelerations under the various load models is given below.

Load case	Accelerations (m/s^2)		
	Allowable	Excitation at 3.3 Hz (vertical mode)	Excitation at 3.7 Hz (torsional mode)
Jogging group	1.89	1.45	1.40
Walking group	1.89	0.70	1.75
Crowd	1.89	0.90	0.25

6.1.1.7 Global buckling analysis

A linear buckling analysis carried out with reference to the ULS1 showed the first significant buckling modes to be essentially local buckling of the deck top panels (see Figure 20). The related buckling load factors are lower than the minimum requested factor of 1.5. However, a geometrical non-linear analysis proved that the local buckling of the top deck panels does not represent an Ultimate Limit State as the bridge deck is still able to stand further increment of the applied loads beyond the minimum amplification factor of 1.5.

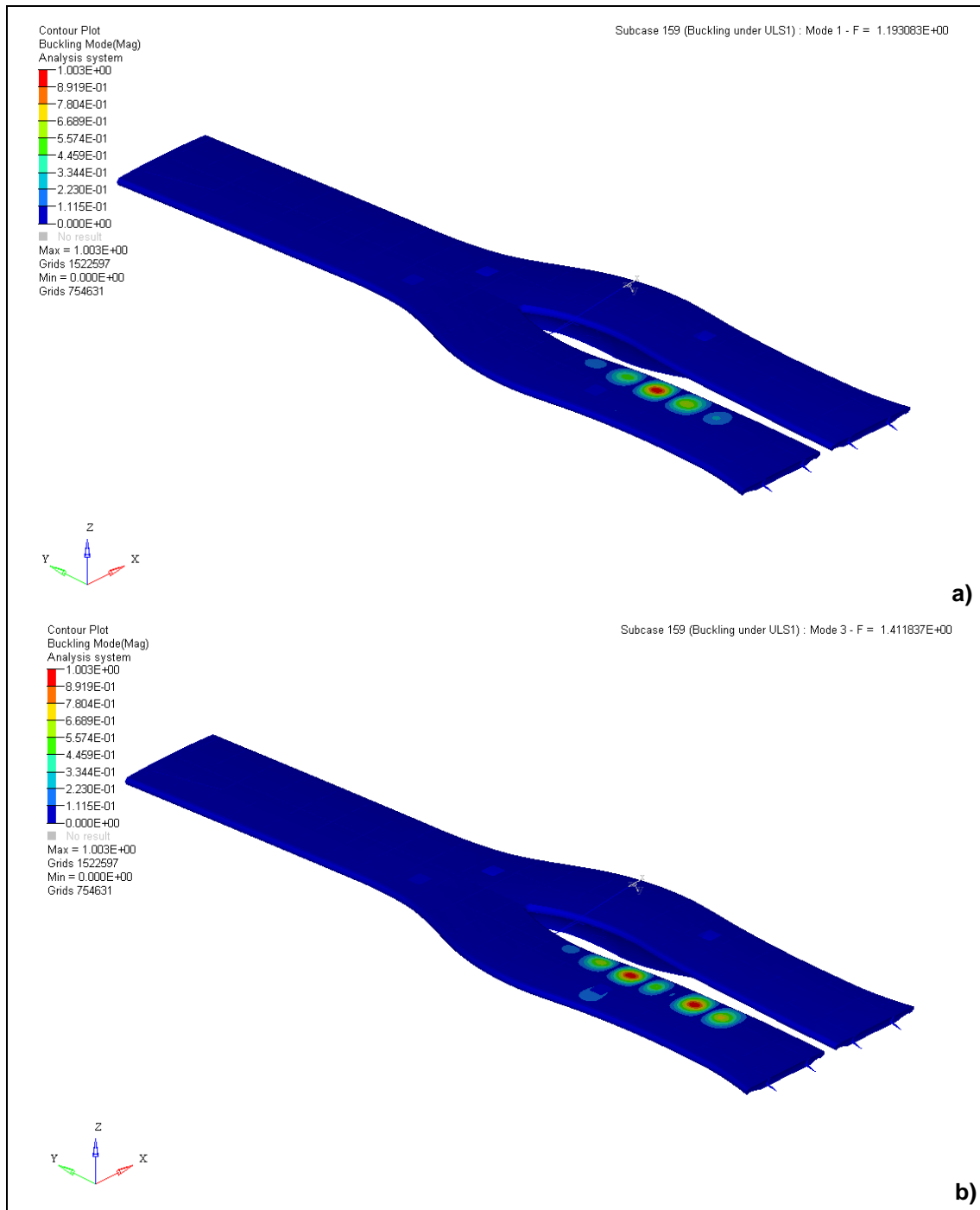


Figure 20: Linear buckling analysis under ULS1: a) first mode; b) second mode

6.1.1.8 ULS1, ULS2 and ULS3 for the check of the composite deck

As it results from the Deck Structural Design Specifications, material partial factors for composites vary not only with the material (laminate, core and adhesive) but also depending on the type of loading, short- or long-term loading. As a consequence, the approach here used when checking the strength of a composite material under a load combination that combines short and long term loadings is to look at the related material partial factors as further equivalent partial load factors. The results reported in the following, referring to the ULS1, ULS2, ULS3 and ULS4 as defined in the Deck Structural Design Specifications [1], will actually account for this approach. Reference should be made to the above document for the adopted material partial factors for composites.

The global check of the strength of the bridge deck in the closed position was carried out with reference to the ultimate load combinations of permanent loads, traffic load and transverse load with the associated downwards load.

The critical load combination is the ULS1, i.e. with traffic load over the entire deck. The following figures show contour plots of the composite failure index (IF) with reference to the maximum strain failure criteria (i.e. maximum ratio between design strain and allowable strain among all the plies of a laminate): Figure 21 refers to the in-plane failure (i.e. ply failure) while Figure 22 refers to inter-lamina shear failure (i.e. core failure). Note that different material partial factors were used for laminates and core as detailed in the design specifications.

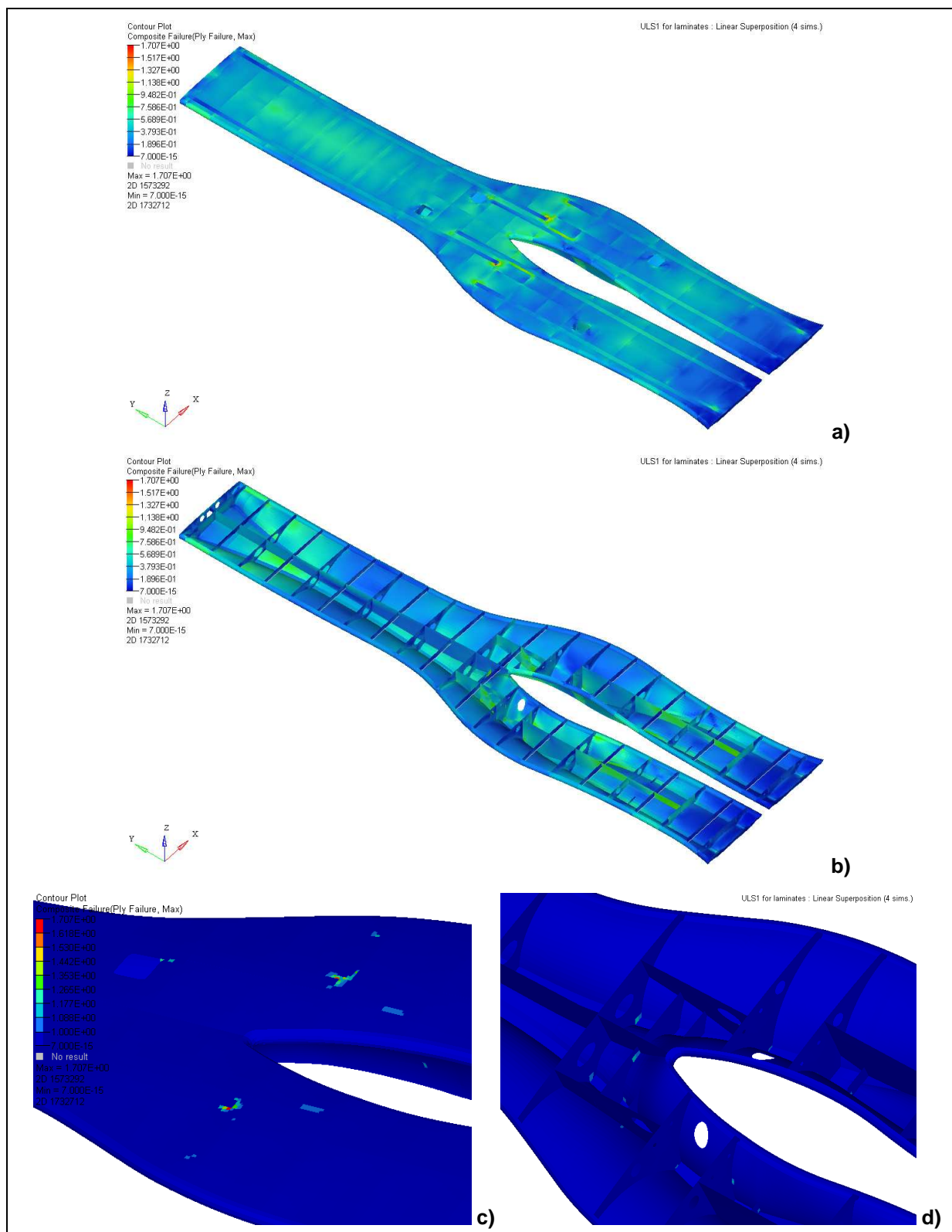


Figure 21: Composite Index Failure Contour at the ULS1 for laminates:
a) Top deck view; b) Soffit and internal structure view;
c) and d) Details with threshold = 1

The plots c) and d), with threshold set at 1.0, indicate local areas where the failure index is over 1.0. However, these localised effects are due to simplifications in the finite element model. For example, stress

concentrations are found at the end of the carbon planks where there is a sudden change in stiffness as the taper of the UD planks is not modelled or at the corner of a hatch as the local reinforcement from the stiffening flange was not modelled. Other elements with failure index (IF) slightly greater than 1 are found along the edge of some bulkheads where the bonding tapes were not modelled. A complete distribution of IF is shown in Figure 21 a) and b).

Figure 22 shows the adequacy of the core material.

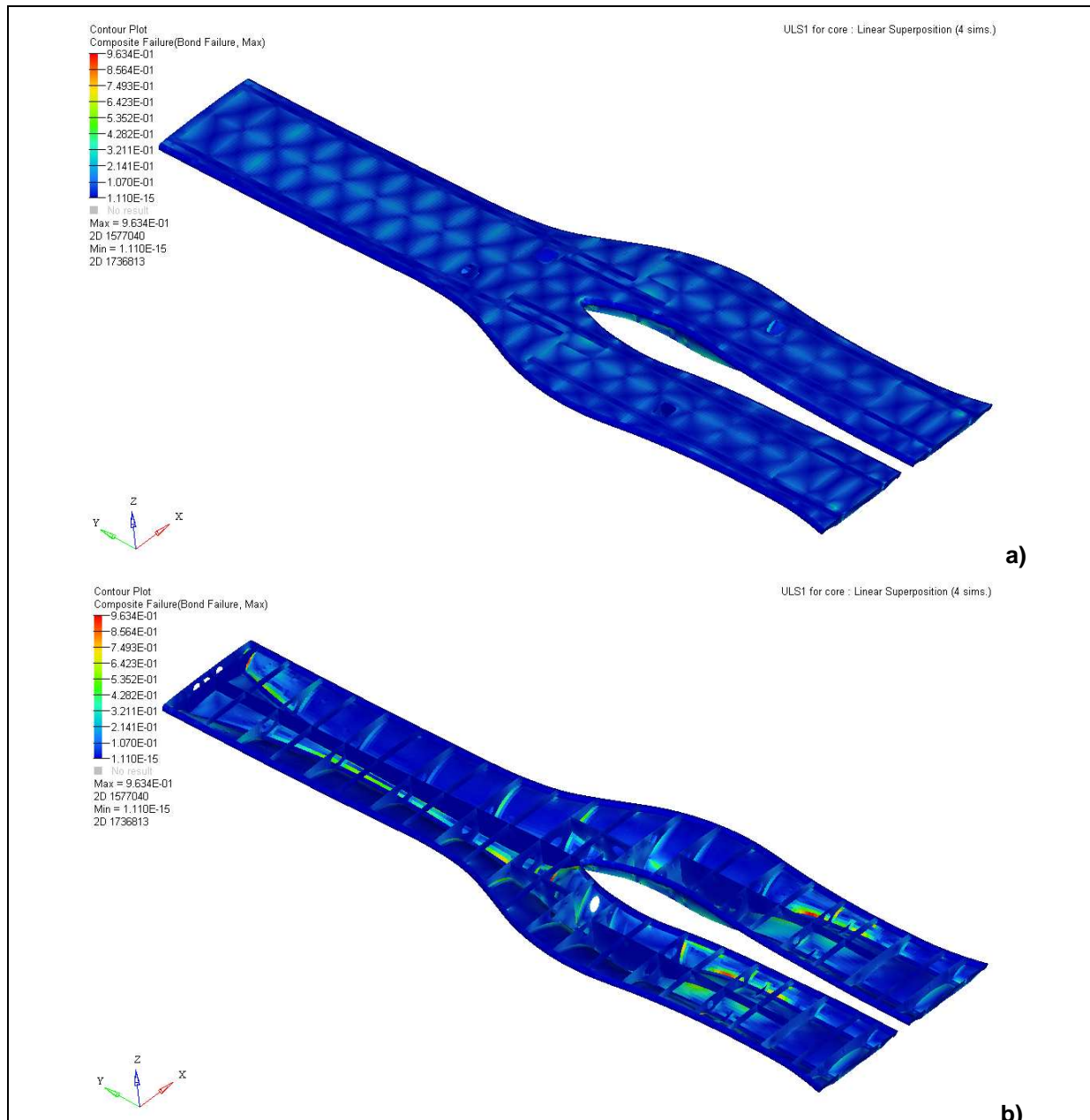


Figure 22: Composite Index Failure Contour at the ULS1 for core:
a) Top deck view; b) Soffit and internal structure view

Once again, some details were actually not modelled like the chamfer of the core where the sandwich panel reduces to a single skin laminates like along the bottom carbon planks. Such a detail behaves like a shear key which locally increases the interlamina shear capacity of the structure.

6.1.1.9 ULS1 to ULS4 for cable and other interfaces

The load combination ULS1 also produced the maximum ultimate force in the lifting/suspension cable equal to:

$$T_{\max,ULS} = 924 \text{ kN}$$

The load combination SLS13, that sees the characteristic combination of permanent loads and transverse wind load with associated uplift wind load, was used to verify the cable remains in tension even in absence of traffic load and with uplift wind. Under that load combination the cable is actually in tension with a force of:

$$T_{\min,SLS} = 130 \text{ kN}$$

The maximum ultimate reactions at the hinge and at the bearings at the tip were found under the ULS1 and are shown in the following figure.

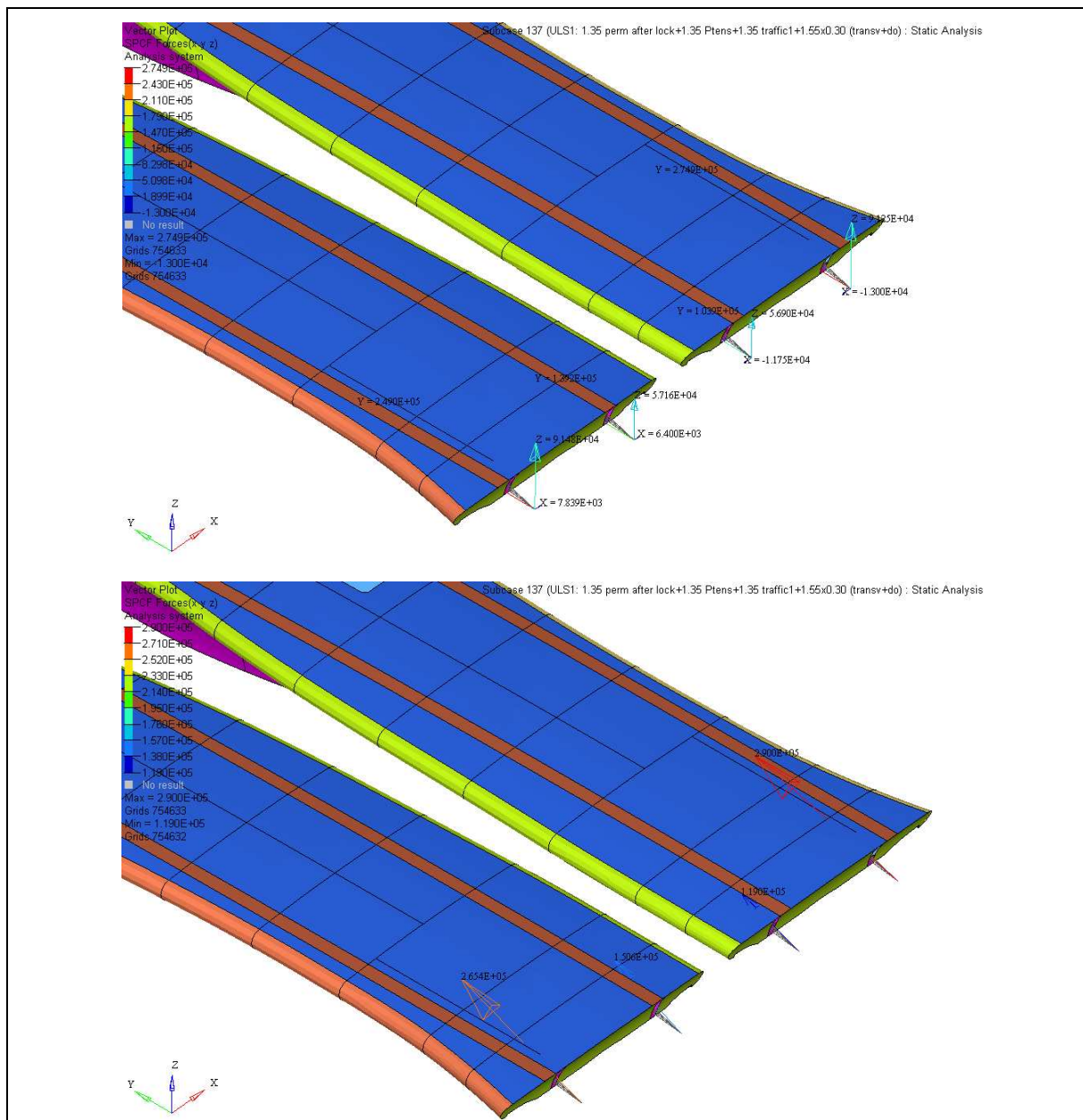


Figure 23: External reactions at the ULS1

6.1.2 Bridge in Partially Open Position

6.1.2.1 Serviceability Limit States

Deflections of the bridge were assessed under permanent load (SLS15) with bridge open at 30° (see Figure 24). The contribution of the downwards/uplift wind associated to the transverse wind and that of the longitudinal wind were also assessed.

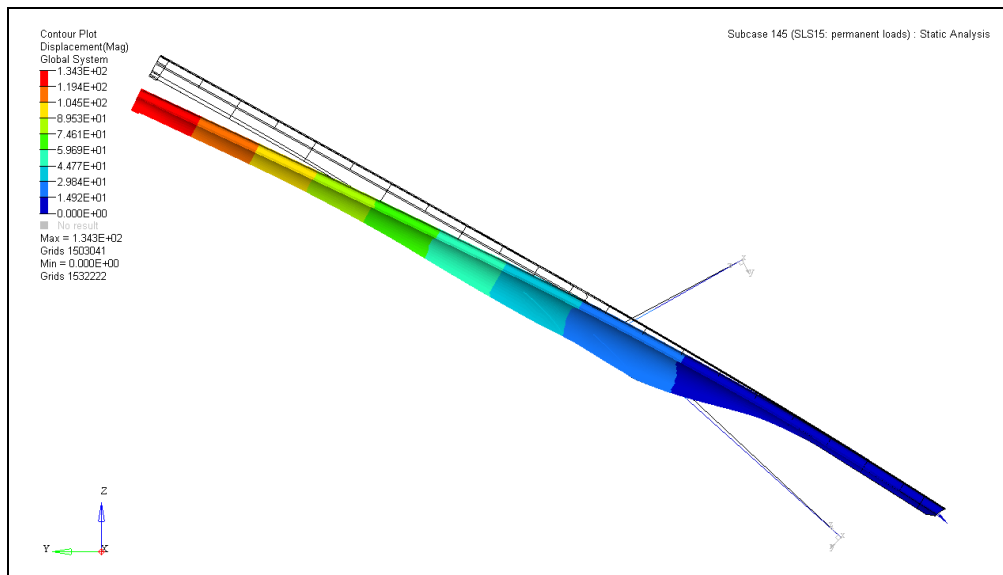


Figure 24: Displacement contour under permanent loads (SLS15) over deformed shape (amplification coefficient 10)

The deflection of the bridge tip under permanent load is 134 mm (i.e. span/239), the contribution of the frequent longitudinal wind load is +/-34 mm whilst that of downwards/uplift wind associated to the transverse wind is +32/-28 mm. The lateral deflection due to frequent transverse wind is 8 mm.

Also note that the cables remain in tension under frequent wind load as well as under characteristic transverse wind and associated uplift wind. On the opposite, under characteristic longitudinal wind load (i.e. corresponding to a wind speed with a probability of 5% to be exceeded in 120 years) the cables will become slack. However, should the cable lose its tension under strong wind this would not be an issue due to the presence of the hydraulic ram which ties the bridge deck down (in closed position the hydraulic ram is not effective).

As per the case of bridge in closed position, in order to reduce the risk of fatigue damage, the resin cracking has been checked under the characteristic combinations of permanent loads, transverse wind with associated downwards/uplift wind (SLS16 and SLS17) and longitudinal wind (SLS18 and SLS19) and the critical results reported in Figure 25.

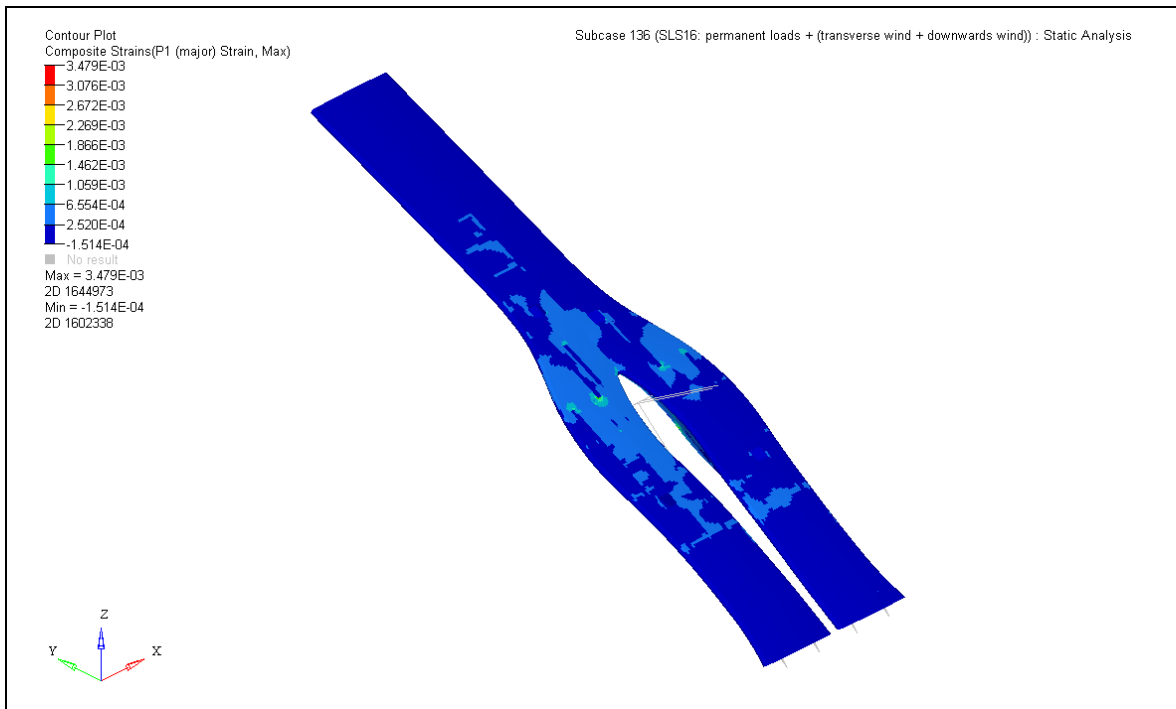


Figure 25: Maximum principal tensile strains contour under characteristic combination SLS16 over deformed shape (amplification coefficient 10)

The maximum principal tensile strains at 0.35% were lower than the limit of 0.4% and therefore no resin cracking is expected. Note that the maximum values were actually concentrated around the hinge as a consequence of a simplified model of the bolt connection.

6.1.2.2 Ultimate Limit States

The global check of the strength of the composite bridge deck in the partially open position was carried out with reference to the ultimate load combinations of permanent loads with transverse wind load and associated downwards/uplift wind load (ULS7 and ULS8) and with longitudinal wind load (ULS9 and ULS10).

The following figures show contour plots of the composite failure index (IF), under the most critical load combinations, with reference to the maximum strain failure criteria (i.e. maximum ratio between design strain and allowable strain among all the plies of a laminate): Figure 26 and 27 refer to the in-plane failure (i.e. ply failure) while Figure 28 refers to inter-lamina shear failure (i.e. core failure). Note that different material partial factors were used for laminates and core (see Par. 6.1.1.9 for more details).

The typical failure index distribution, with reference to the ply failure, is shown in Figure 26, under the ULS7.

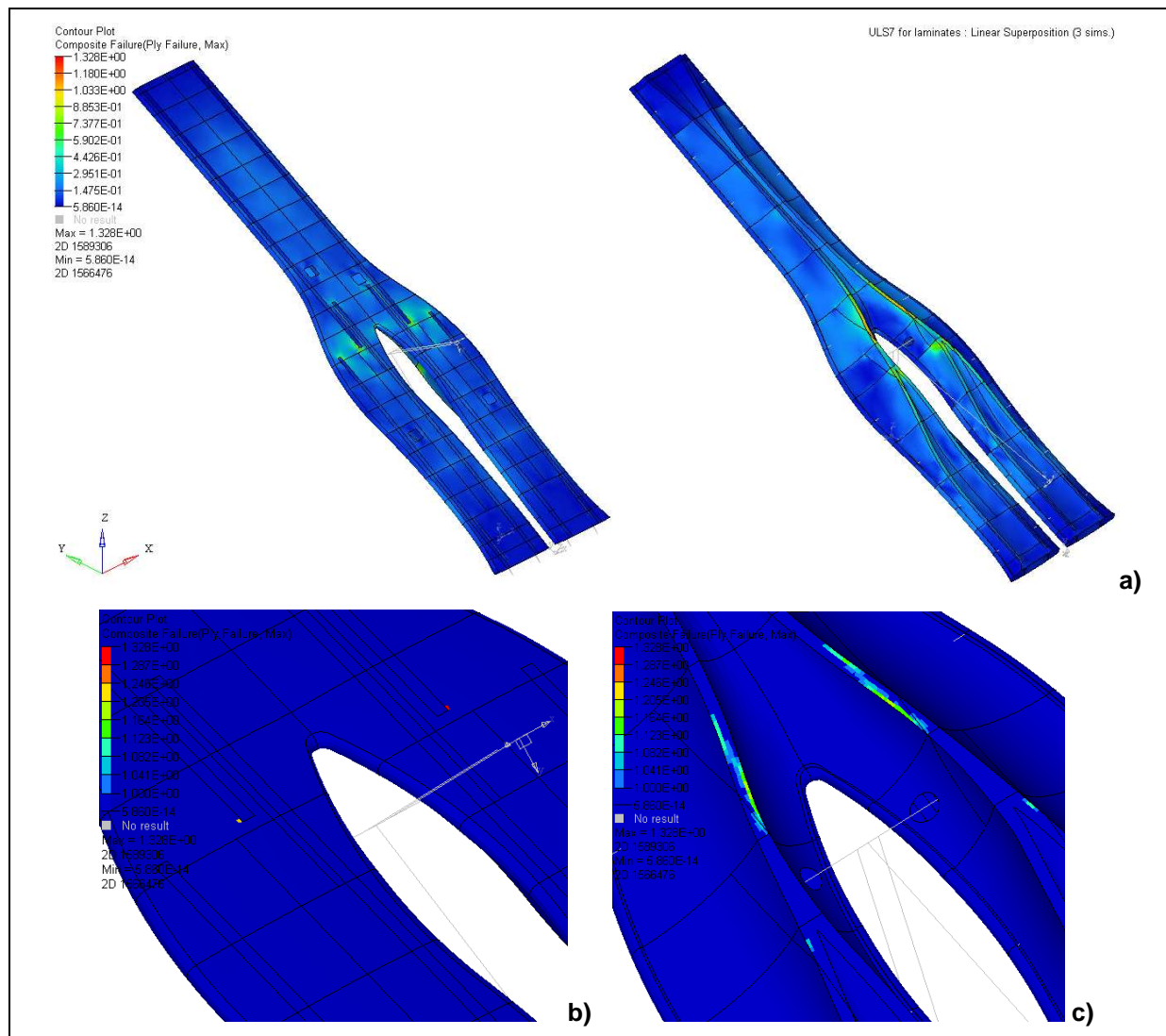


Figure 26: Composite Index Failure Contour at the ULS7 for laminates:
a) Top and bottom deck view; b) and c) Details with threshold = 1

The plots b) and c), with threshold set at 1.0, highlight spots where the failure index is above 1. In particular, Figure 26 c) reveals a failure index above 1.0 for resin cracking in the transverse direction of the UD carbon planks. In this case transverse resin cracking of the UD is not considered an ultimate failure, due to the presence of the QE990 and the intermediate plies of XE900 between the plies of UD.

Note that, while the local failure shown in the Figure 27 b) (ULS 10) is due to the modelling simplification of the end of the tapes as detailed for the closed bridge case. The local failure indicated in figure 27(c) occurs in a region where there is additional reinforcement from the bonding of the longitudinal which is not included in the model, so the strength of the laminate is considered to be acceptable.

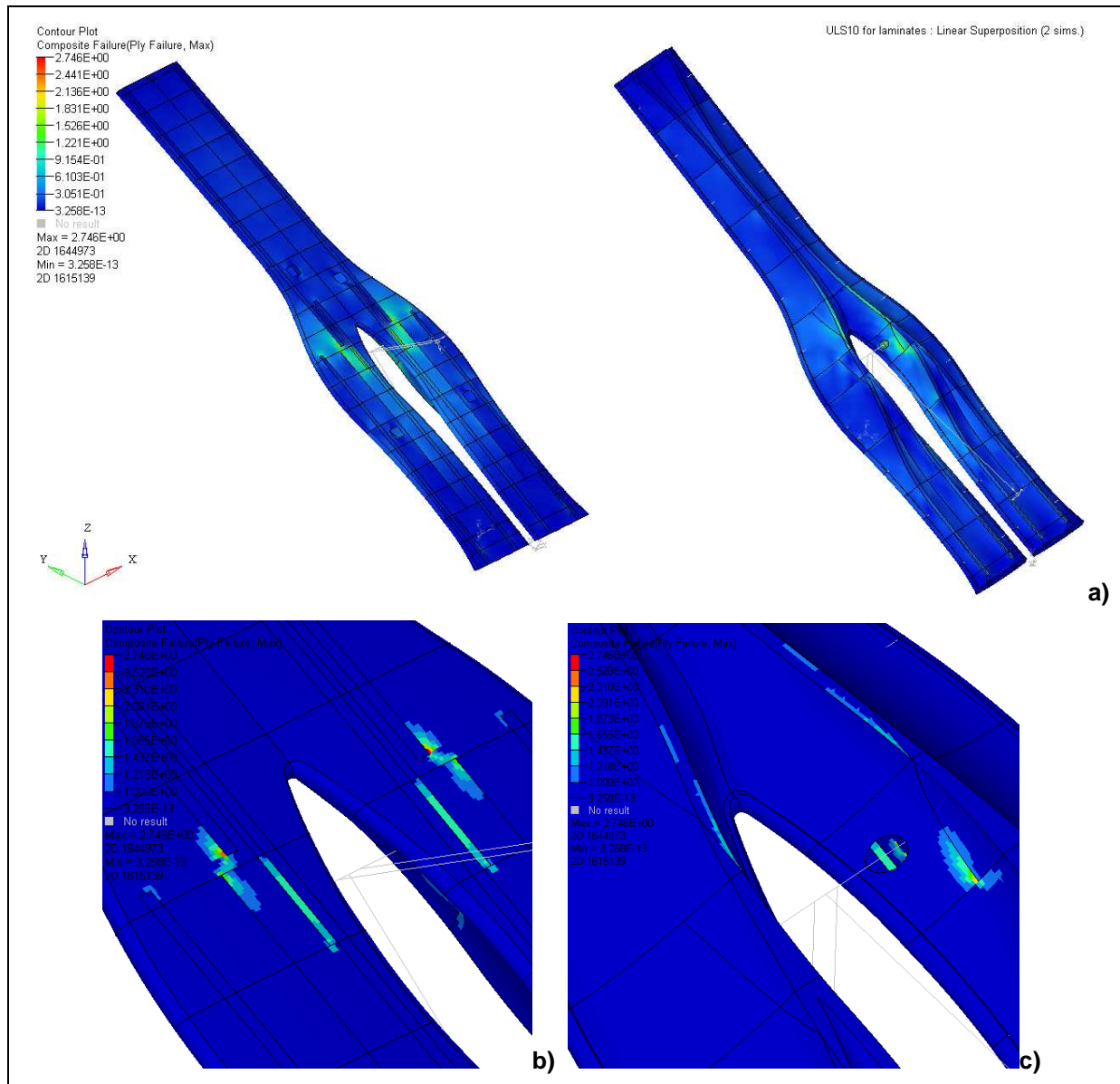


Figure 27: Composite Index Failure Contour at the ULS10 for laminates:
a) Top and bottom deck view; b) and c) Details with threshold = 1

In Figure 28 the failure index contour plot for the core is reported for the most critical load combination (ULS10) and it shows the adequacy of the core material.

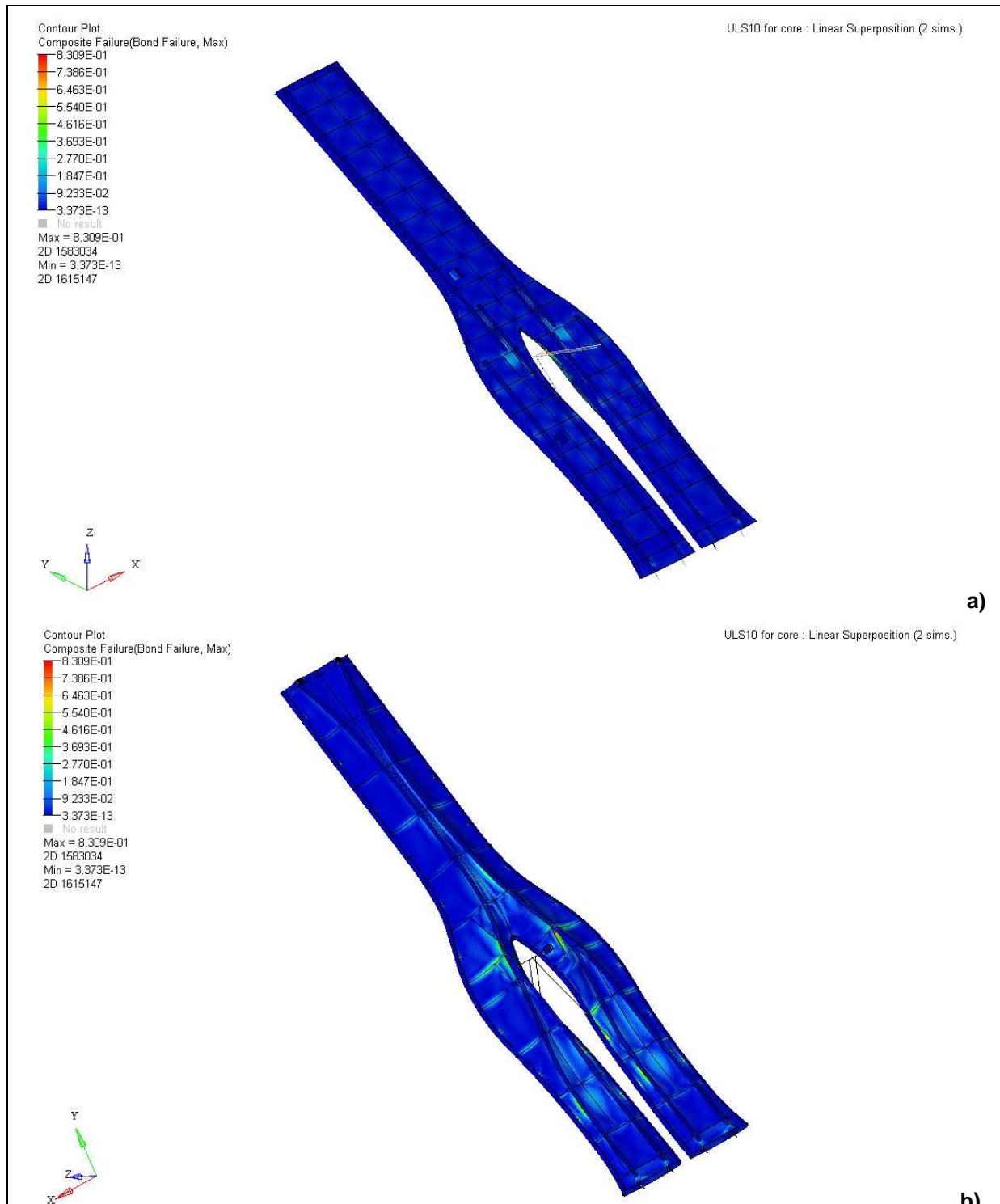


Figure 28: Composite Index Failure Contour at the ULS10 for core:
a) Top deck view; b) Soffit view

Once again, for simplicity some details were actually not modelled in the global model, like the chamfer of the core where the sandwich panel reduces to a single skin laminates like along the bottom carbon planks. Such a detail behaves like a shear key which locally increases the interlamina shear capacity of the structure.

6.1.3 Bridge in Fully Open Position

6.1.3.1 Serviceability Limit States

The deflection of the tip of the bridge under permanent loads reduces to 70 mm, respect to the case of partially open bridge. On the other hand, the contribution of the frequent longitudinal wind pressure increases to +/-51. The load case with transverse wind was not significantly different to the transverse wind case under the partial open condition. The longitudinal wind case was critical for the fully open position, and so the transverse wind load condition was not analysed for the fully open bridge. Under frequent longitudinal wind load the cables remain in tension with the bridge in fully open position, while under characteristic wind the cables become slack.

The resin cracking has been checked under the characteristic combinations of permanent loads and longitudinal wind (SLS21 and SLS22) and the critical results reported in Figure 29.

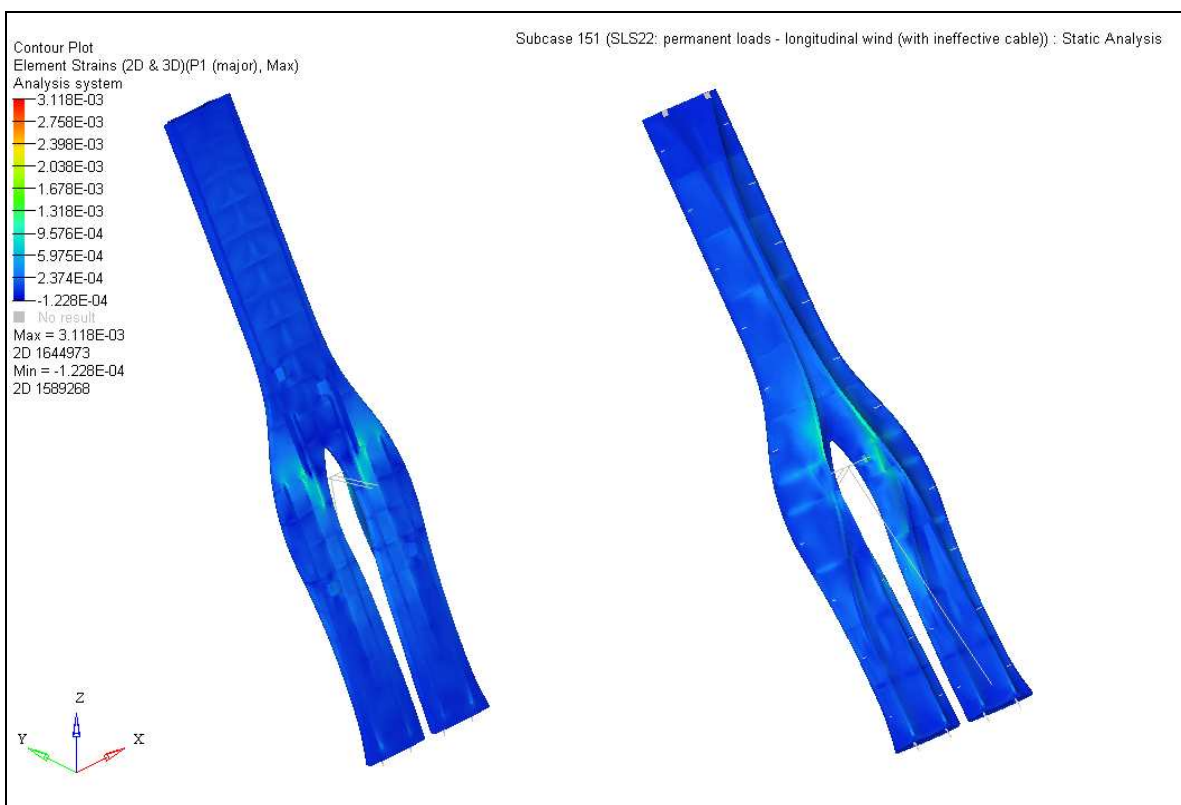


Figure 29: Maximum principal tensile strains contour under characteristic combination SLS22

The maximum principal tensile strains of 0.31% were lower than the design limit of 0.4% and therefore no resin cracking is expected. Note that the maximum values were actually concentrated around the hinge as a consequence of a simplified model of the bolt connection.

6.1.3.2 Ultimate Limit States

Similarly to the case of partially open bridge, load combinations in ultimate conditions with longitudinal wind load (ULS11 and ULS12) were investigated in order to verify the global strength of the composite bridge deck. The load case with transverse wind was not critical for the fully open case and was not analysed.

The following figures show contour plots of the composite failure index (IF), under the most critical load combinations, with reference to the maximum strain failure criteria (i.e. maximum ratio between design strain and allowable strain among all the plies of a laminate): Figure 30 refers to the in-plane failure (i.e. ply failure) under the ULS11, while Figure 31 refers to inter-lamina shear failure (i.e. core failure) under the ULS12. Note that different material partial factors were used for laminates and core (see Par. 6.1.1.9 for more details).

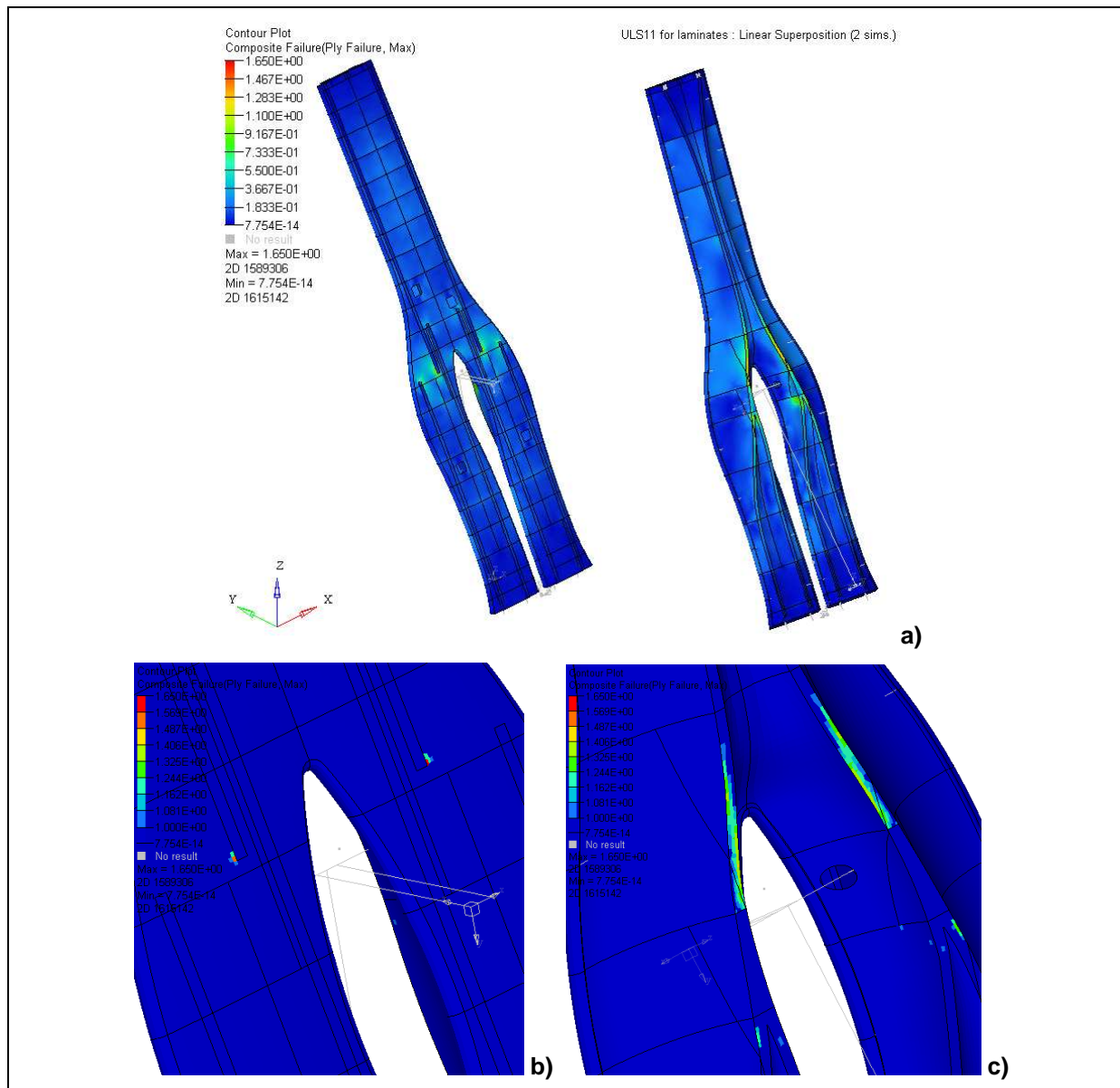


Figure 30: Composite Index Failure Contour at the ULS11 for laminates:
a) Top and bottom deck view; b) and c) Details with threshold = 1

The same comments made for the case of partially open bridge (Par. 6.1.2.2) apply here to the localized areas with IF>1 shown in the plots b) and c).

In Figure 31 the IF contour plot is reported for the most critical load combination (ULS12) and it shows the adequacy of the core material.

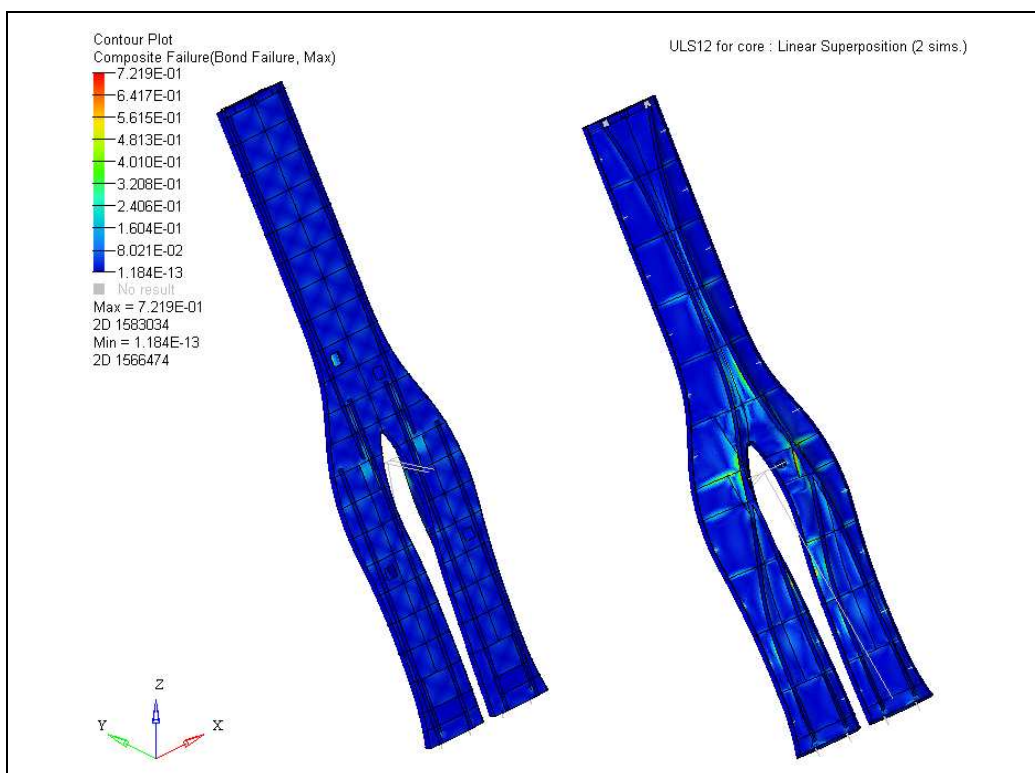


Figure 31: Composite Index Failure Contour at the ULS12 for core

6.2 Local Analysis of the Deck

The top deck is supported by transverse bulkheads 3 m spaced. In addition transverse stiffeners are located between the transverse bulkheads. A longitudinal diaphragm divides the 4 m wide deck in two.

Local deflections of the deck under pedestrian load (i.e. 5 kN/m²) and service vehicle were assessed by modelling a portion of the bridge deck between four consecutive bulkheads along the landward side span. Simple supports were introduced under the bulkheads in order to isolate the local displacements (i.e. differential displacements) of the top deck (see Figure 32).

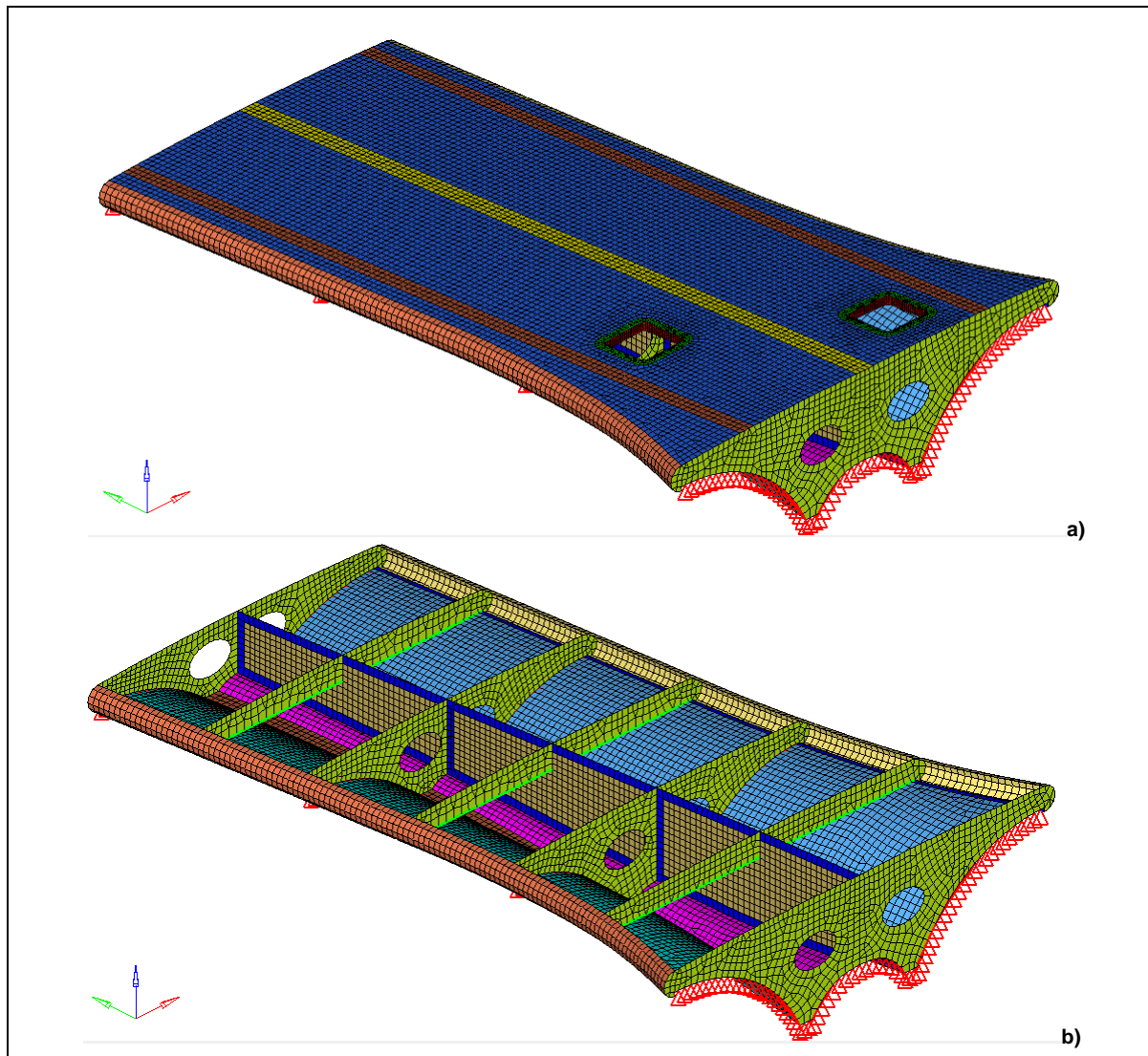


Figure 32: FE Model for local deflections of the deck under traffic loads:
a) top view; b) internal structure

Different traffic load distributions were investigated (see Figure 33) and the deflections at the central portion assumed as representative of the typical local deflections of the deck bridge.

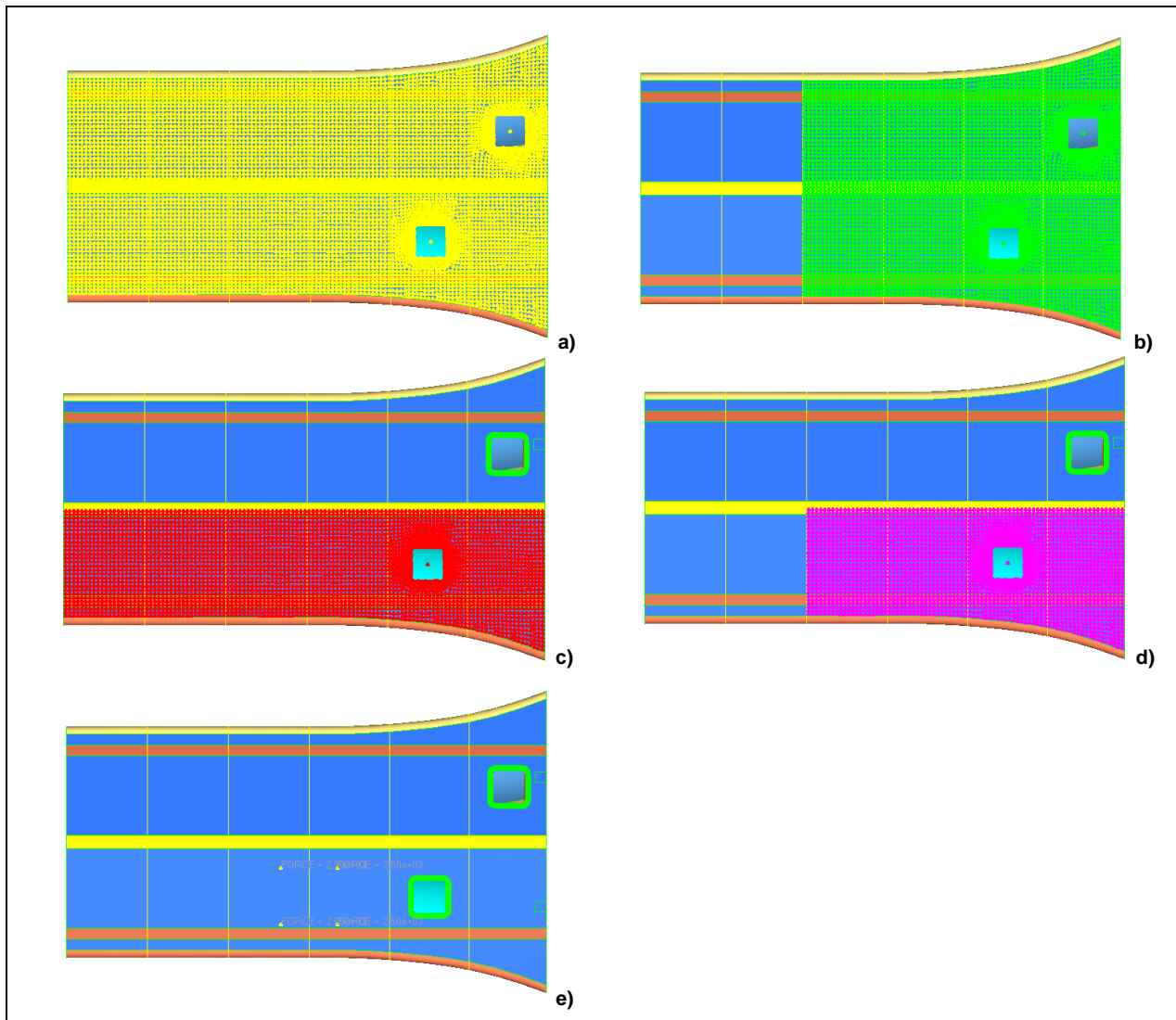
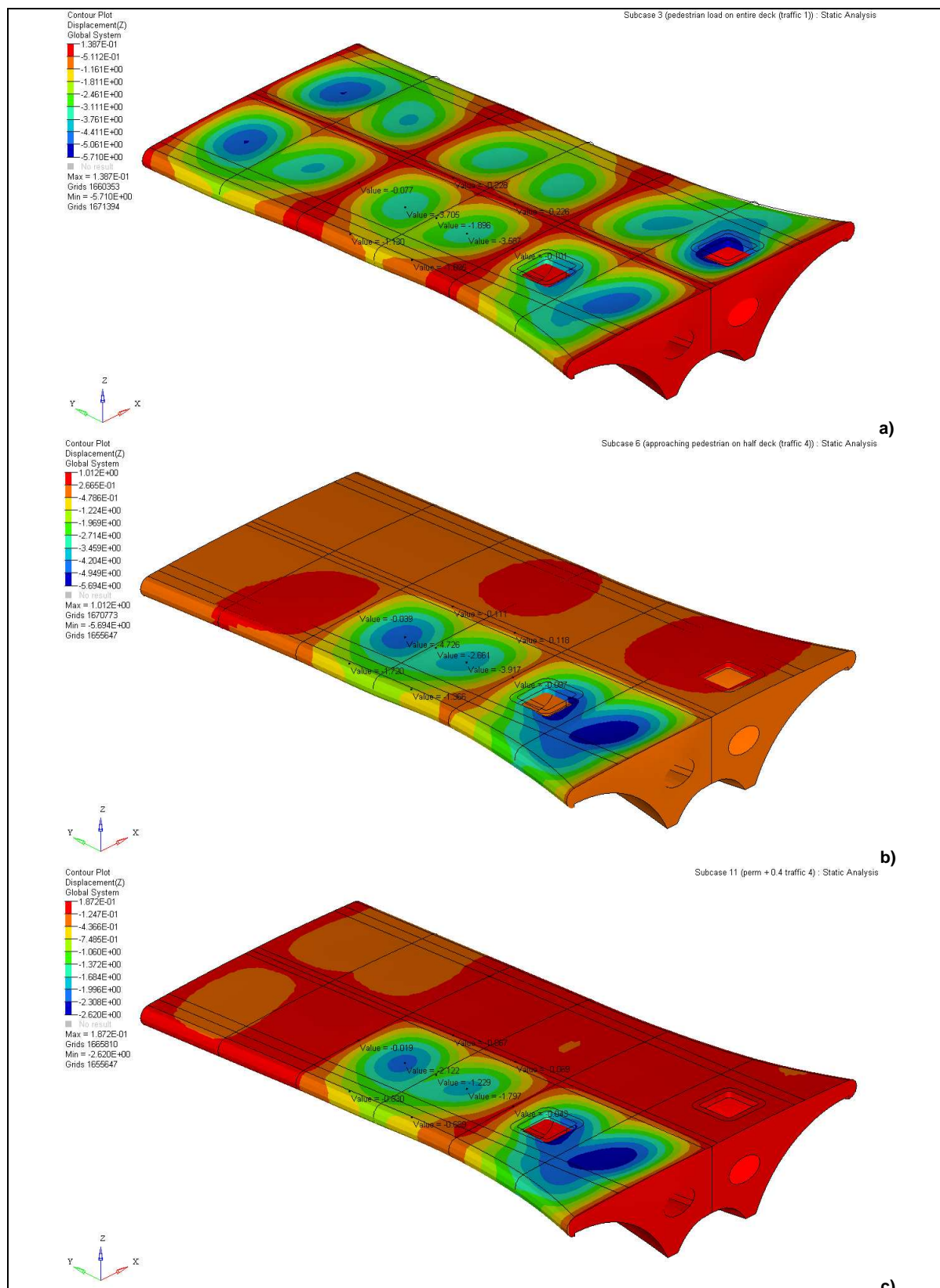


Figure 33: Traffic loads distributions:

- a) pedestrian load on entire deck (traffic 1);
- b) approaching pedestrian on entire deck (traffic 2);
- c) pedestrian load on half deck (traffic 3)
- d) approaching pedestrian on half deck (traffic 4)
- e) service vehicle

Figure 34 shows three examples of vertical displacement contour over a deformed shape under traffic load. The maximum relative displacement resulted under the load distribution "traffic 4": under characteristic load the local deflection was equal to 3.4 mm with reference to the longitudinal direction (i.e. span/444 with span = 1500 mm) and to 3.8 mm with reference to the transverse direction (i.e. span/525 with span = 2000 mm). The plot in Figure 34 c) refers to the SLS for reversible load combination required by the Eurocode with permanent loads plus frequent value of traffic load (i.e. 0.40 characteristic value). These deflections are considered acceptable.



**Figure 34: Contour of displacements over deformed shape (amplification coefficient 20):
a) characteristic traffic 1; b) characteristic traffic 4;
c) permanent + 0.40 traffic 4.**

The case of service vehicle was not significant in terms of deflection and was considered for the check of core under concentrated load. Assuming the wheel load of 2.5 kN acting over an area of 100x100 mm², for the check of punching failure the shear stress is:

$$\tau = \gamma_L \gamma_m F / (t \times 4b) = 1.35 \times 1.50 \times 2500 / (40 \times 400) \text{ N/mm}^2 = 0.32 \text{ N/mm}^2 < \tau_{\text{allowable}} = 0.96 \text{ N/mm}^2 (\text{RF}=3)$$

The contact pressure is:

$$p = \gamma_L \gamma_m F / b^2 = 1.35 \times 1.50 \times 2500 / 100^2 \text{ N/mm}^2 = 0.51 \text{ N/mm}^2 < \sigma_{\text{allowable}} = 0.53 \text{ N/mm}^2 (\text{RF}=1.05)$$

6.3 Design of Bridge Details

The design and check of details are reported in the following paragraphs. Essentially these were carried out by means of the analysis of simplified and conservative local models, based on assumptions commonly adopted and on the output of the FE analysis of the global model.

6.3.1 Interface at the hinge end

The structural arrangement at the interface between the composite deck and the steel works at the hinge end of the bridge is shown in Figure 35, containing extracts from the construction drawings.

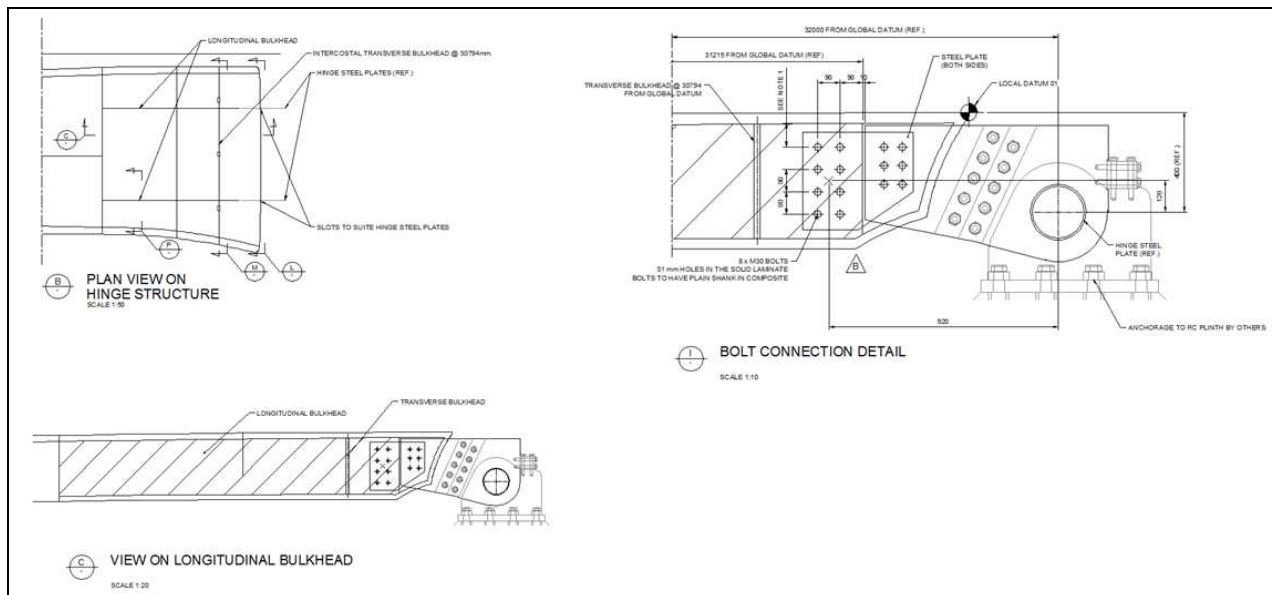


Figure 35: Structural arrangement

The critical ULS load combination is the ULS1, with pedestrian load over the entire deck. With reference to the material partial factors for steel structural design, the longitudinal and vertical components at the hinge are respectively (see Figure 36):

$$R_l = 275 \text{ kN}$$

$$R_v = 91 \text{ kN}$$

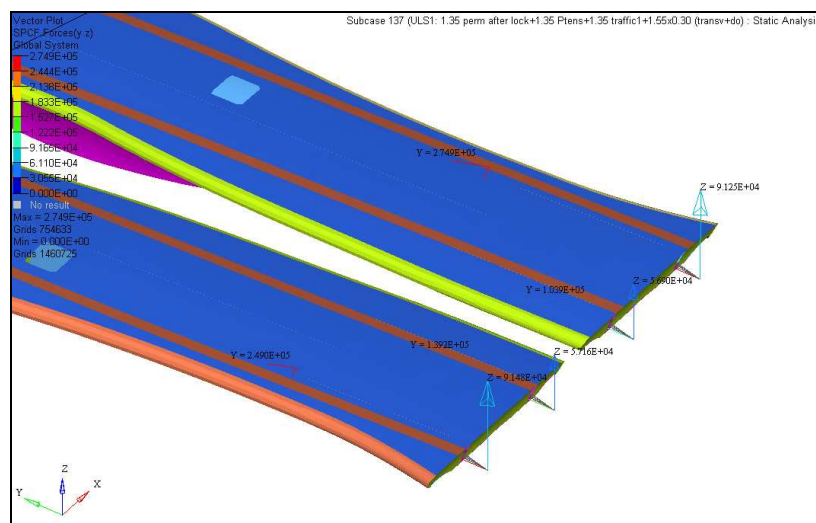


Figure 36: Reactions at the ULS1 for steel design

and the corresponding maximum shear force in the bolts, taking into account that bolts work in double shear, is:

$$F_{V,Ed} = 108/2 \text{ kN} = 54 \text{ kN}$$

For bolts M30 Class 8.8, the shear resistance is:

$$F_{V,Rd} = 210 \text{ kN}$$

(see Figure 37)

Therefore:

$$F_{V,Ed} = 54 \text{ kN} < F_{V,Rd} = 210 \text{ kN} \quad (\text{RF}=3.9)$$

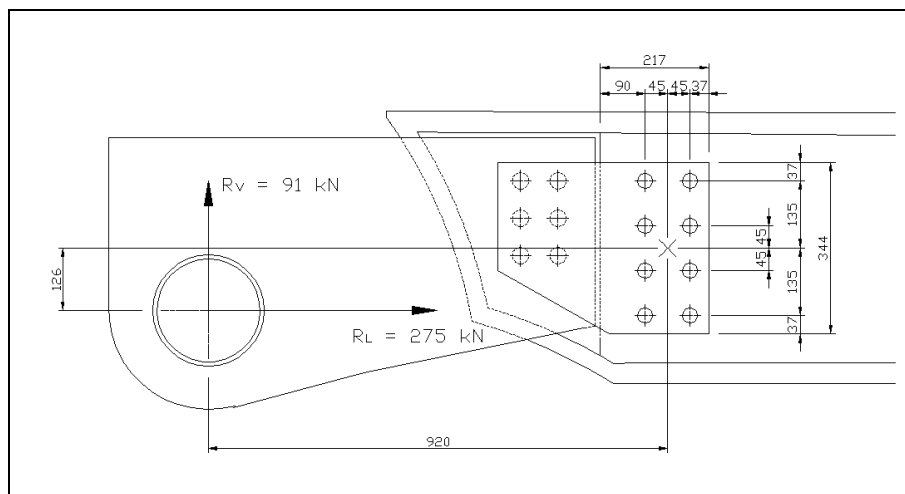


Figure 37: Scheme for bolt connection

Assuming the two steel plates 25 mm thick (note that the interfacing steel plate was indicated as 50 mm) and of Class S355, the bearing resistance is (using the notation adopted by the Eurocode):

$$\begin{aligned} F_{b,Rd} &= k_1 a_b f_u d t / \gamma_{M2} = \\ &= 1.48 \times 0.45 \times 510 \text{ N/mm}^2 \times 30\text{mm} \times 25\text{mm} / 1.25 = 226.7 \text{ kN} < F_{V,Ed} = 54 \text{ kN} \quad (\text{RF}=4.2) \end{aligned}$$

The steel plates can be considered adequate.

The laminate of the longitudinal bulkhead is defined in Figure 38.

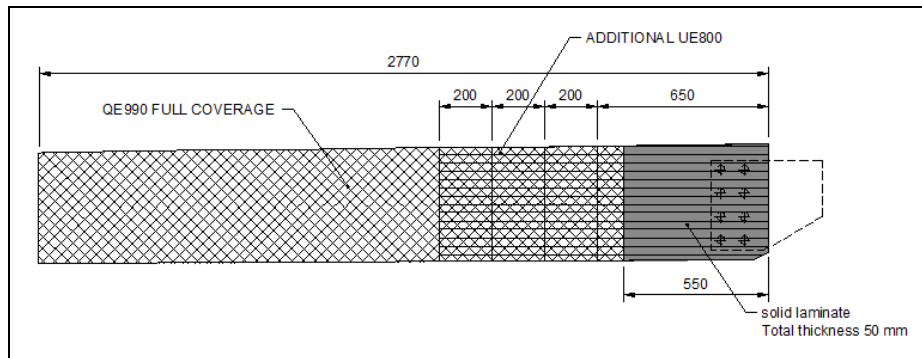


Figure 38: Laminate of longitudinal bulkhead

With reference to the design of laminate materials in bearing, the longitudinal and vertical components at the hinge are respectively:

$$R_l = 704 \text{ kN}$$

$$R_v = 164 \text{ kN}$$

and the corresponding maximum shear force in the bolts, taking into account that bolts work in double shear, is:

$$F_{V,Ed} = 180/2 \text{ kN} = 90 \text{ kN}$$

Hence, the bearing pressure on the 50 mm solid glass laminate is:

$$\sigma_b = 2 \times 90 \times 10^3 \text{ N} / (30\text{mm} \times 50\text{mm}) = 120 \text{ N/mm}^2 < \sigma_{b,a} = 200 \text{ N/mm}^2 \quad (\text{RF} = 1.6).$$

In assessing the resistance to the net section failure, we referred to the longitudinal component of the hinge reaction, being this in the order of 2.5 times bigger than the vertical component and also being the geometry of the connection more vulnerable in that direction (see Figure 39). The longitudinal component of the hinge reaction at the ULS1 for laminate materials is:

$$R_l = 900 \text{ kN}$$

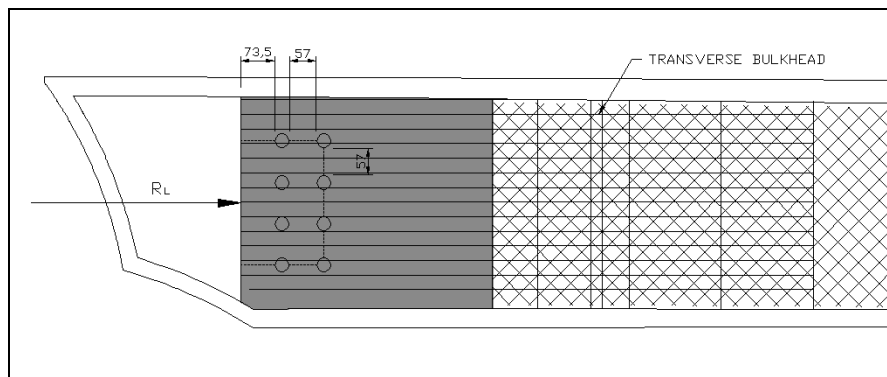


Figure 39: Net section in the solid laminate at the bolt connection

The shear resistance along the two horizontal surfaces and the compressive resistance over the front surface are respectively equal to:

$$F_{S,Rd} = \tau_{ip,a} \times A_{res} = 156 \text{ N/mm}^2 \times 2 \times (73.5+57) \text{ mm} \times 50 \text{ mm} = 2036 \text{ kN}$$

$$F_{C,Rd} = \sigma_{c,a} \times A_{res} = 197.9 \text{ N/mm}^2 \times 3 \times 57 \text{ mm} \times 50 \text{ mm} = 1692 \text{ kN}$$

Both the two components of the resistance to the net section failure are individually able to resist the applied load (RF = 1.9).

QE990 has been used for the basic laminate of the longitudinal bulkheads. The amount of glass was assessed as that required to transfer in shear the horizontal component R_l of the reaction from the hinge to the top deck and soffit and the vertical component R_v to the transverse bulkhead. 6 plies of QE990 per skin were specified over the entire length of the bulkhead.

Considering a conservative length of $L = 600 \text{ mm}$ for the purpose of transferring the horizontal reaction R_l , the shear stress in the two skins is:

$$\tau = R_l / (4L \times 6t) = 900000 \text{ N} / (4 \times 600 \text{ mm} \times 6 \times 0.86 \text{ mm}) = 72.7 \text{ N/mm}^2 < \tau_{ip,a} = 156 \text{ N/mm}^2 \quad (\text{RF}=2.1)$$

With a double-side bonding of 4xXE900 per side to the top deck and soffit, the shear stress in the bonding laminate is:

$$\tau = R_l / (4L \times 4t) = 900000 \text{ N} / (4 \times 600 \text{ mm} \times 4 \times 0.83 \text{ mm}) = 113 \text{ N/mm}^2 < \tau_{ip,a} = 130 \text{ N/mm}^2 \quad (\text{RF}=1.15)$$

Similarly, the vertical component R_v induces a shear stress per skin:

$$\tau = R_v / (2H \times 6t) = 216000 \text{ N} / (4 \times 440 \text{ mm} \times 6 \times 0.86 \text{ mm}) = 23.8 \text{ N/mm}^2 < \tau_{ip,a} = 156 \text{ N/mm}^2 \quad (\text{RF}=6.5)$$

and with a four-side bonding of 2xXE900 per side to the transverse bulkhead, the shear stress in the bonding laminate is:

$$\tau = R_v / (4H \times 2t) = 216000 \text{ N} / (4 \times 440 \text{ mm} \times 2 \times 0.83 \text{ mm}) = 74 \text{ N/mm}^2 < \tau_{ip,a} = 130 \text{ N/mm}^2 \quad (\text{RF}=1.75)$$

As shown in Figure 38, UE tapes have been added in order to promote the diffusion of the concentrate load from the bolt connection along the longitudinal bulkhead. The amount of UE800 has been assessed as that required to be alone capable to stand in compression the entire longitudinal load. The 4xUE800 per skin are subjected to a compressive stress of:

$$\sigma = R_l / (2H \times 4t) = 900000 \text{ N} / (2 \times 440 \text{ mm} \times 4 \times 0.7 \text{ mm}) = 365 \text{ kN/mm}^2 < \sigma_c = 398 \text{ N/mm}^2 \quad (\text{RF}=1.1)$$

The UE types have been actually extended over 1 m and staggered by 250 mm per ply in order to reduce the stress concentration at the end.

6.3.2 Lifting pin support structure

The structural arrangement for the lifting pin support structure is shown in Figure 40, containing extracts from the construction drawings.

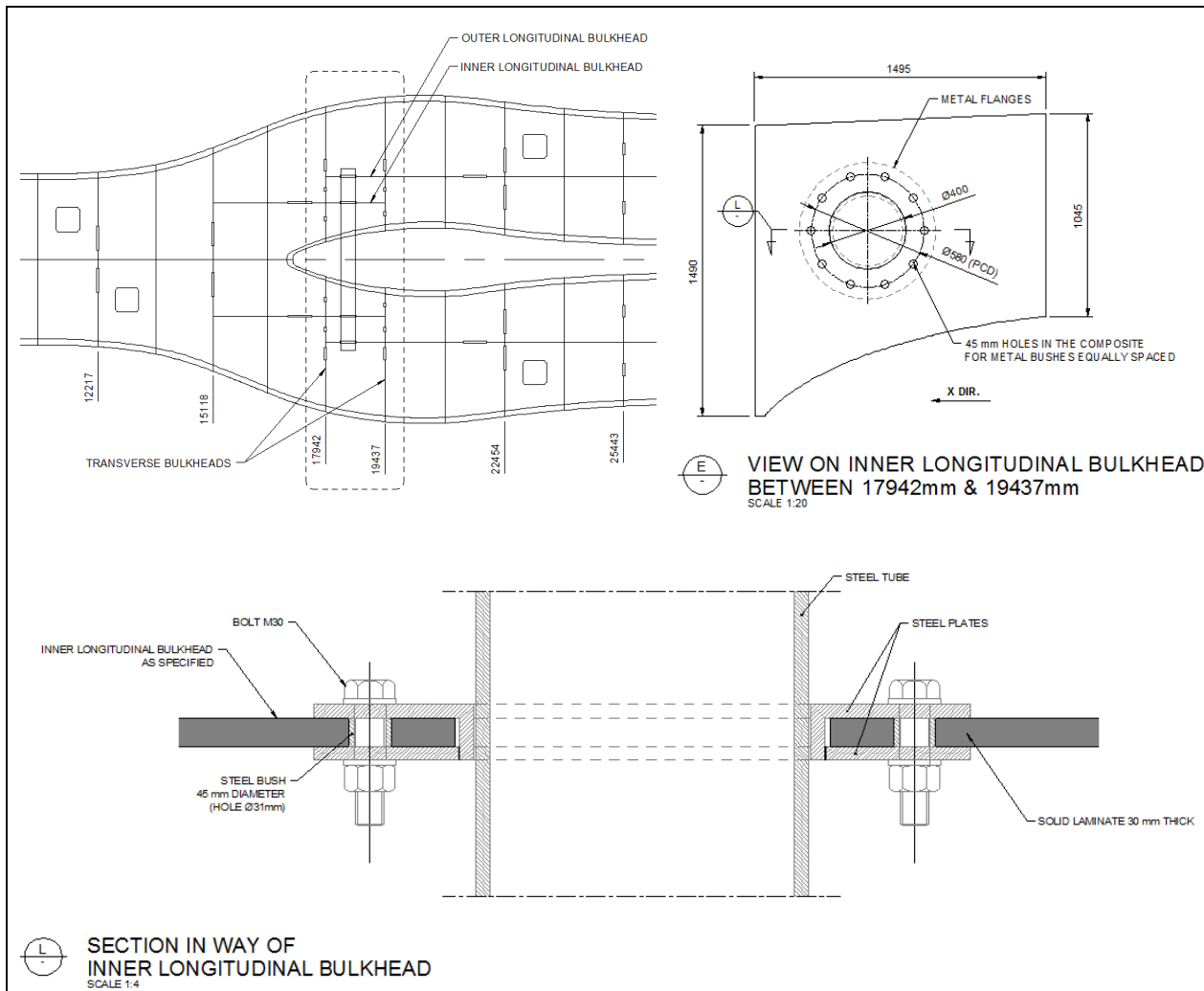


Figure 40: Structural arrangement

Essentially, the composite bridge deck is supported at the mid span by a steel tube, in turn connected to steel cables suspended from the mast. The steel tube passes through four longitudinal composite bulkheads. The interface consists of a system of steel flanges bolted to the bulkheads, with the load transferred in bearing through the bolts.

The critical ULS load combination is the ULS1, with pedestrian load over the entire deck, and the most loaded longitudinal bulkheads are the inner ones. With reference to the material partial factors for steel structural design, the longitudinal and vertical components at the interface between inner bulkheads and steel lifting tube are (see Figure 41):

$$R_l = 605 \text{ kN}$$

$$R_v = 310 \text{ kN}$$

with reference to the material partial factors for laminates:

$$R_l = 2080 \text{ kN}$$

$$R_v = 1250 \text{ kN}$$

with reference to the material partial factors for laminates in bearing:

$$R_l = 1630 \text{ kN}$$

$$R_v = 990 \text{ kN}$$

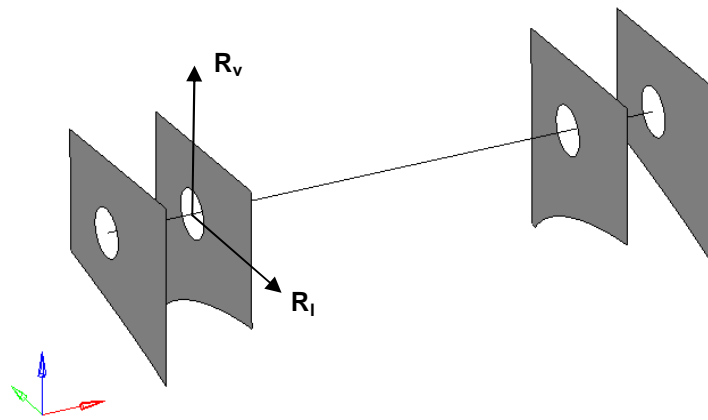


Figure 41: Reactions at the ULS1 for steel design

With reference to the bearing resistance of the 30 mm solid E-plate, the maximum shear force per bolt is:

$$F_{V,Ed} = 1/10 \times (1630^2 + 990^2)^{0.5} \text{ kN} = 190 \text{ kN}$$

and the corresponding bearing pressure:

$$\sigma_b = 190 \times 10^3 \text{ N} / (30\text{mm} \times 45\text{mm}) = 140 \text{ N/mm}^2 < \sigma_{b,a} = 200 \text{ N/mm}^2 \quad (\text{RF}=1.40).$$

Note that in the above calculation the assumption of the steel flanges sufficiently rigid to be able to distribute the load equally between the 10 bolts was made. The resulting reserve factor will largely cover any difference with the actual distribution.

Being the bulkheads entirely made from solid E-plate and given their dimensions and the layout of the connection, the bulkhead capacity is driven by the bearing capacity checked above. This was confirmed by the analysis of the FE model.

For the check of the bonding of the longitudinal bulkheads to the transverse bulkheads, given the stiffness of the solid bulkheads, a uniform distribution of shear stresses is assumed along the bonding. In particular, with reference to the material partial factors for laminates, the shear stress due to the vertical component of the reaction R_v is:

$$\tau = R_v / (H \times 8t) = 1250000 \text{ N} / [(1490+1045)\text{mm} \times 8 \times 0.83\text{mm}] = 74 \text{ N/mm}^2 < \tau_{ip,a} = 130 \text{ N/mm}^2 \quad (\text{RF}=1.75)$$

with the bonding consisting of 4xXE900 each side.

The shear stress due to the horizontal component of the reaction R_l is:

$$\tau = R_l / (L \times 8t) = 2080000 \text{ N} / (2 \times 1495\text{mm} \times 8 \times 0.83\text{mm}) = 105 \text{ N/mm}^2 < \tau_{ip,a} = 130 \text{ N/mm}^2 \quad (\text{RF}=1.24)$$

References

- [1] Foryd Harbour Bridge - Deck Structural Design Specifications (Report No. 3073-8000), Gurit
- [2] BS EN 1990:2002+A1:2005, Basis of structural design
- [3] NA to BS EN 1990:2002+A1:2005
- [4] BS EN 1991-2:2003, Traffic loads on Bridges
- [5] NA to BS EN 1991-2:2003
- [6] EuroComp Design Code and Handbook for Structural Design of Polymer Composites,
The European Structural Polymeric Composite Group, 1996
- [7] Foryd Harbour Sustainable Transport Bridge – Deck Loading Report;
Report No. 15621/REP/DL/01 Rev A by Ramboll
- [8] Train Buffeting Measurements on a Fibre-Reinforced Plastic Composite Footbridge,
Structural Engineering International, Volume 21, Number 3, August 2011, pp. 285-289(5) by Santos, M.
and Mohan, M.

Bibliography

- An Introduction to Sandwich Construction, Dan Zenkert, EMAS Publishing, 1997
- Mechanical Testing of Advanced Fibre Composites, J. M. Hodgkinson, Woodhead Publishing Limited 2000
- Design Manual for Roads and Bridges, Volume 1, Section 3 Part 17 BD90/05: Design of FRP Bridges and Highway Structures